

Empirical stream thermal sensitivities cluster on the landscape according to geology and climate

Lillian M. McGill¹, E. Ashley Steel², Aimee H. Fullerton³

¹Center for Quantitative Sciences, University of Washington, Seattle, WA 98105, USA, ORCID ID: 0000-0003-2722-2917

²School of Aquatic and Fishery Sciences, University of Washington, Seattle, WA 98105, USA, ORCID ID: 0000-0001-5091-276X

³Northwest Fisheries Science Center, National Oceanic and Atmospheric Administration, 2725 Montlake Blvd. East, Seattle, WA 98112, USA, ORCID 0000-0002-5581-3434

Correspondence to: Lillian M. McGill (lmcgill@uw.edu)

Abstract

Climate change is modifying river temperature regimes across the world. To apply management interventions in an effective and efficient fashion, it is critical to both understand the underlying processes causing stream warming and identify the streams most and least sensitive to environmental change. Empirical stream thermal sensitivity, defined as the change in water temperature with a single degree change in air temperature, is a useful tool to characterize historical stream temperature conditions and to predict how streams might respond to future climate warming. We measured air and stream temperature across the Snoqualmie and Wenatchee basins, Washington during hydrologic years 2015-2021. We used ordinary least squares regression to calculate seasonal summary metrics of thermal sensitivity and time-varying coefficient models to derive continuous estimates of thermal sensitivity for each site. We then applied classification approaches to determine unique thermal sensitivity regimes and, further, to establish a link between environmental covariates and thermal sensitivity regime. We found a diversity of thermal sensitivity responses across our basins that differed in both timing and magnitude of sensitivity. We also found that covariates describing underlying geology and snowmelt were the most important in differentiating clusters. Our findings can be used to inform strategies for river basin restoration and conservation in the context of climate change, such as identifying climate insensitive areas of the basin that should be preserved and protected.

1 Introduction

Globally, river temperature regimes are shifting in response to a changing climate. As water temperature is a critical component of aquatic ecosystems, these changes will alter an essential element of the habitat of many lotic organisms (Daufresne and Boët 2007). To apply management interventions in an effective and efficient fashion, it is critical to both understand the underlying processes causing stream warming (Arismendi et al. 2014, Steel et al. 2017) and identify the streams most and least sensitive to environmental change (Parkinson et al. 2016, Pyne and Poff 2017, Jackson et al. 2018).

34 Both deterministic and statistical models have been used to study water temperature (Caissie 2006, Dugdale
35 et al. 2017, Ouellet et al. 2020). Physical process-based models balance energy (heat) and mass (flow) fluxes in a
36 water body (Glose et al. 2017). Process-based approaches allow the identification of the most important drivers in the
37 heat budget of streams across timescales, improving the resolution and accuracy of stream temperature predictions
38 (Stefan and Sinokrot 1993, van Beek et al. 2012, Wondzell et al. 2019). Issues exist with process-based modelling,
39 however, including intensive data and computational needs (e.g., spatially distributed land use and soil characteristics,
40 meteorological and discharge data, etc.), limited ability to generalize across basins, and difficulty representing
41 groundwater and subsurface flow paths (Safeeq et al. 2014). Statistical models are computationally simpler with
42 potentially minimal data requirements (Benyahya et al. 2007) facilitating prediction at ecologically relevant spatial
43 grains and extents. These models are appealing because of their simplicity and limited requirement of meteorological
44 and hydraulic data, while still being characterized by high levels of explained variance in some basins. However, it
45 can be difficult to derive insights about river response to perturbations from statistical models as statistical approaches
46 rely on historical relationships that may not extrapolate well to future conditions. For example, relationships may
47 change between water temperature and covariates such as discharge or the composition and coverage of riparian
48 vegetation and land use. Statistical models would therefore benefit from a clearer understanding of the relationships
49 between derived model coefficients and important watershed processes.

50 Empirical stream thermal sensitivity, defined as the change in water temperature with a single degree change
51 in air temperature, or the slope of the statistical relationship between air temperature and water temperature, has been
52 widely used to characterize historical stream temperature conditions and to predict how streams might respond to
53 future climate warming (Mohseni et al. 2003, Mantua et al. 2010). Thermal sensitivities reflect the combined influence
54 of both spatially and temporally varying meteorological and hydrological factors. Variation in solar radiation is the
55 most important driver of both air and river temperature, and as a result, air and river temperatures are typically
56 correlated (Johnson 2003). Stream temperature is also influenced by discharge through changes to thermal inertia and
57 residence time (Meier et al. 2003) and runoff composition where snowmelt, surface runoff, or groundwater inflow
58 entering the stream have different temperature signatures than the stream itself (Webb and Zhang 1997, Mohseni and
59 Stefan 1999). Inputs from water sources such as snowmelt and groundwater upwelling decouple air and water
60 temperatures and result in a decreased thermal sensitivity of water temperature to air temperature (Tague et al. 2007,
61 Mayer 2012, Johnson et al. 2014). As a result, the relationship between air and water temperature can also be a useful

62 diagnostic tool for hydrological processes. Thermal sensitivity has been used in the past to estimate areas of shallow
63 and deep groundwater influence (Snyder et al. 2015, Briggs et al. 2018) and understand the role of snowmelt in
64 modulating river temperature (Lisi et al. 2015, Winfree et al. 2018).

65 Generally, larger thermal sensitivities indicate that water temperatures are more likely to track changes in air
66 temperature (Isaak et al. 2016, Mauger et al. 2017, Isaak et al. 2018b); however, there are concerns about employing
67 this approach to predict future stream temperatures. Past studies have found that using empirical relationships for
68 extrapolating to future climate scenarios without accounting for underlying processes such as snowmelt, groundwater,
69 and annual hysteresis may provide inaccurate predictions of future stream temperatures (Leach and Moore 2019, Steel
70 et al. 2019). Under changing climatic conditions, the interrelations between air temperature and other processes
71 controlling stream temperature may not remain stable (Arismendi et al. 2014). Additionally, stream networks can
72 exhibit patchy thermal conditions due to spatially heterogeneous landscape attributes such as riparian shading, valley
73 form and aspect, and geology (Bogan et al. 2003, Benyahya et al. 2010). Large-scale models that do not incorporate
74 fine-scale variation in thermal sensitivity may not accurately predict thermal habitat at ecologically relevant scales.
75 Despite these shortcomings, thermal sensitivity remains a commonly used and straightforward tool that allows for
76 comparison between locations within rivers and has the potential to guide management.

77 There is a need to better understand how thermal sensitivities evolve throughout the year and along river
78 networks. A clearer vision of how thermal sensitivities vary will allow managers to understand what a single snapshot
79 in time or space represents and could provide insight into how river thermal sensitivity may evolve under nonstationary
80 air temperature and precipitation regimes. Identification of groups of streams that share similar patterns of thermal
81 sensitivity will also have management relevance. Groups of streams with similar thermal sensitivities will likely also
82 share similar risk profiles; managers may therefore tailor investment in streams within groups based on watershed
83 specific influences (Mayer 2012). This study aims to answer three questions across two Pacific Northwest river basins:
84 **1) What is the spatial and temporal distribution of commonly used air-water temperature metrics across each basin?**
85 **2) What are the representative regimes of air-water temperature correlations, how do they cluster on the landscape,**
86 **and how do these clusters differ from clusters based solely on air and water temperature? and 3) What are the landscape**
87 **or climate factors that best predict cluster membership?**

88 2 Methods

89 2.1 Study Area

90 The Snoqualmie River begins as three distinct forks in the Mt. Baker Snoqualmie National Forest and drains a 1,813
91 km² watershed on the west side of the Cascade Range, Washington (Figure 1). The three forks originate in forested
92 public land before converging and flowing through a mix of agricultural, residential, and commercial land use. On
93 one major tributary, the Tolt River, a dam and a large reservoir provide drinking water for the City of Seattle (Figure
94 S4). The Wenatchee River drains 3,440 km² of the eastern Cascades before flowing into the Columbia River (Figure
95 S5). Although land use is similar to the Snoqualmie basin, wherein the headwaters originate in forested public lands
96 before flowing through a mix of agricultural, residential, and commercial land use, forest density is generally lower
97 in the eastern Cascades.

98 Both the Snoqualmie and Wenatchee basins have a Mediterranean climate with dry summers and wet, mild
99 winters influenced by proximity to the Pacific Ocean. The climate on the east side of the Cascades is drier than that
100 of the west side; however, the prevailing westerly winds, which cross the Cascades, create temperature and
101 precipitation gradients that vary widely across the Wenatchee basin. Precipitation occurs predominately from October
102 to March. The coldest month is typically January, whereas the warmest is July. Rivers have a mixed rain-snow
103 hydrology with substantial winter rain and spring snowmelt, although the Wenatchee basin receives a greater
104 proportion of winter precipitation as snow. Peak flow generally occurs during winter in the Snoqualmie River and
105 spring in the Wenatchee River (Figure 2). The Snoqualmie and Wenatchee basins both have reaches where water
106 temperature exceeds regulatory thresholds established for salmonids that are protected by the U.S. Endangered Species
107 Act (ESA). Both basins support ESA-listed Chinook Salmon (*Oncorhynchus tshawytscha*) and Steelhead Trout
108 (*Oncorhynchus mykiss*) and the Wenatchee basin additionally supports populations of Bull Trout (*Salvelinus*
109 *confluentus*) and Sockeye Salmon (*Oncorhynchus nerka*).

110 Water temperature loggers ($N_{\text{Snoqualmie}}=42$, $N_{\text{Wenatchee}}=31$) were installed throughout the mainstems, on major
111 tributaries and on a selection of minor tributaries for both the Snoqualmie and Wenatchee rivers (Figure 1). Practical
112 limitations forced sites to be publicly accessible, or on private property with landowner permission, and within 1 km
113 of a road. For this study, water temperature was recorded using HOBO TidbiT v2 (UTBI-001) loggers every hour
114 from October 1, 2014 through September 30, 2021 in both basins. We hereafter use North American hydrologic years
115 (1 October – 30 September) instead of calendar years with the year of summer data as the year of reference. Air

116 temperature data was recorded using HOBO Pendant (UA-002-64) loggers at all water temperature monitoring sites.
117 Air temperature was logged for subset of 11 (6) sites in the Snoqualmie (Wenatchee) basin beginning October 1, 2014,
118 and for all sites beginning October 1, 2016 (October 1, 2018). Air loggers were placed on trees along the stream bank,
119 as close to the stream temperature loggers as possible. The air temperature loggers were secured at approximately
120 breast height on the north side of the trees. Solar shields were fashioned to house both water and air temperature
121 loggers.

122 **2.2 Exploratory analysis of air-water correlation summary metrics**

123 We calculated two summary metrics to characterize the relationship between air temperature and water temperature.
124 For each site, summary metrics were derived from linear regressions between mean daily values of air and water
125 temperature. The slope of this relationship, the thermal sensitivity, indicates the average difference in water
126 temperature when comparing time periods with a one-degree difference in air temperature. For example, a thermal
127 sensitivity of 0.5 would indicate that, based on historical data, when air temperature at a site differs by 1°C, water
128 temperature differs on average by 0.5°C (Leach and Moore 2019). The strength of this relationship (R^2) is an indicator
129 of how well water temperature can be approximated by air temperature and is calculated as the Pearson correlation
130 value between air and water temperature. Summary metrics were calculated separately for each season. Seasons were
131 defined as fall (October, November, December), winter (January, February, March), spring (April, May, June), and
132 summer (July, August, September).

133 A large body of literature examines landscape-level drivers of air and water temperature correlations within
134 rivers. Therefore, we first summarized hypothesized drivers of thermal sensitivity based on previous literature and
135 their covarying landscape variables within our basins. We then conducted an exploratory analysis of the relationship
136 between landscape covariates and thermal sensitivity to better understand patterns in our data and set up future
137 hypothesis testing. Due to the correlated nature of our dataset, no formal statistical tests were conducted. We plotted
138 summer thermal sensitivity against hypothesized drivers, including mean watershed elevation (MWE), watershed
139 slope, distance upstream, percent riparian forest cover, and substrate hydraulic conductivity. Loess curves were plotted
140 to aid in data visualization, and correlation coefficients between thermal sensitivity and each landscape covariate were
141 used to quantify the strength of the linear relationship. Covariate descriptions and sources are found in Table 1.

142 We also explored the relationship between spring thermal sensitivity and snowmelt, defined as the change in
143 Snow Water Equivalent (SWE) for a given season, and between summer thermal sensitivity and mean air temperature

144 and total precipitation. Climatic variables were obtained from gridded DAYMET data products (Thornton, M.M. et
145 al. 2020) and calculated for the upstream catchment of each monitoring station.

146 **2.3 Spatially weighted clustering of thermal sensitivity, water temperature, and air temperature**

147 To identify representative regimes of air-water temperature correlations, we employed a varying-coefficient linear
148 model to obtain continuous, daily estimates of thermal sensitivity. We then defined a spatially weighted dissimilarity
149 matrix for use in clustering, which quantifies the spatial correlation in thermal sensitivity time series while accounting
150 for the directed river network structure. We used this spatially weighted dissimilarity matrix with agglomerative
151 hierarchical clustering to identify groups of sites exhibiting similar patterns in thermal sensitivity over time and
152 compared these clusters to those generated using only water or air temperature. Details of each step are provided in
153 the following sections.

154 **2.3.1 Varying coefficient linear model for air-water relationship**

155 To derive a continuous thermal sensitivity metric, we fit a time-varying coefficient model (TVCM) to air and water
156 temperature data. The TVCM is an effective tool for exploring dynamic features of the sensitivity of water temperature
157 with changes in air temperature and uses a parametric linear model but with time-varying coefficients (Li et al. 2014,
158 2016). For a given site, we described the varying coefficient model for the air–water temperature relationship as:

$$159 \quad y_t = \beta_{0,t} + x_t \beta_{1,t} + \epsilon_t, t = 1, \dots, T \quad (1)$$

160 Where $\beta_{0,t}$ and $\beta_{1,t}$ are varying intercept and slope coefficients. To estimate the time-varying coefficients, we adopted
161 an ordinary least squares kernel regression with the Nadaraya–Watson estimator, where we fit a set of weighted local
162 regressions with an optimally chosen window size defined by the bandwidth, b , and the weights given by the kernel
163 function (Hoover 1998, Casas and Fernandez-Casal 2019). The kernel and its bandwidth control the level of smoothing
164 by adjusting the weight that the neighbouring time points have on estimates at t . The bandwidth was set to 0.2 a priori
165 to ensure consistency across time series. We used the Gaussian kernel that is of the form $k(x) = \frac{1}{2} \pi e^{-\frac{x^2}{2}}$. The varying
166 intercept term represents the mean water temperature at time t and the varying slope term represents the local
167 sensitivity of water temperature to changes in air temperature at time t . We used the R package tvReg (Casas and
168 Fernandez-Casal 2021) for implementing the model.

169 We filtered resultant time series for site-years with > 218 days (60% of the year) and gaps of ≤ 7 days,
170 yielding 250 site-years from 74 sites across both the Snoqualmie and Wenatchee basins. To capture the typical range

171 and timing of thermal sensitivity at each site, we created a single representative time series of thermal sensitivity at
 172 each site by calculating the mean daily thermal sensitivity for each day of the year across all years of filtered data. We
 173 use this average annual time series for subsequent clustering analyses. To ensure that using an average annual time
 174 series of thermal sensitivity was an appropriate choice given the structure of our data, we conducted a supplementary
 175 analysis to assess cluster sensitivity to interannual variability (Appendix A).

176 **2.3.2 Estimating a spatially weighted dissimilarity matrix**

177 To quantify spatial correlation while accounting for the directed river network structure, we developed a dissimilarity
 178 measure for time series of thermal sensitivity, water temperature, and air temperature that incorporated spatial
 179 correlation between sites (Haggarty et al. 2015). The general form of the proposed dissimilarity measure between sites
 180 x and y can be written as:

$$181 \quad d_{xy}^c = d_{xy} \widehat{cov}(h_s) \quad (2)$$

182 where d_{xy}^c is the spatially weighted dissimilarity matrix, d_{xy} is the Canberra distance (Lance and Williams 1967), and
 183 $\widehat{cov}(h_s)$ is a valid stream distance-based covariance matrix.

184 To estimate $\widehat{cov}(h_s)$, we used the tail-down model that was introduced by Ver Hoef and Peterson (2010).
 185 Due to the complex structure of the tail-down model, it is necessary to model spatial correlation on a river network
 186 with a covariogram. We first estimated the covariance between time series at each site using a classic formula from
 187 Cressie (1993), which states that the estimated covariance between sites x and y is given by

$$188 \quad \widehat{cov}(x, y) = \sum_{t=1}^T \frac{\{x_t - \bar{x}\}\{y_t - \bar{y}\}}{T} \quad (3)$$

189 where x_t and y_t are the values of the variable (thermal sensitivity, water temperature, or air temperature) at sites x and
 190 y at time t and T is the total number of discrete times. This results in a single value which summarizes the covariance
 191 between the time series at the two sites over the period of interest. We then plotted these point summaries of the
 192 covariance between pairs of curves against lags (measured as stream distance) to obtain an empirical stream distance-
 193 based covariogram. We fit an exponential covariance function to this empirical covariogram and evaluated the model
 194 at relevant distances to obtain an estimated stream distance-based covariance matrix $\widehat{cov}(h_s)$. We used this new
 195 covariance matrix to weight the Canberra distance matrix as shown in Equation 2. The final spatially weighted
 196 dissimilarity matrix, d_{xy}^c , was then used in clustering analyses.

197 **2.3.3 Agglomerative hierarchical clustering**

198 We used agglomerative hierarchical clustering (AHC) to identify groups of sites where the patterns in thermal
199 sensitivity, water temperature, and air temperature were similar over time using the hclust function in R (R Core Team
200 2020). AHC is a common clustering method (Olden et al. 2012, Maheu et al. 2016, Savoy et al. 2019, Isaak et al.
201 2020) where each time series starts in its own cluster, and the hierarchy is built by repeatedly merging pairs of similar
202 clusters separated by the shortest distance (i.e., measured as the similarity between individual times series) until all
203 points are contained in a single cluster. To decide which clusters are merged in every iteration, AHC uses a dissimilarity
204 metric (d_{xy}^c , derived in Equation 2) and a linkage criterion. We used Ward's minimum variance linkage method for
205 clustering, where the distance between two clusters is computed as the increase in the sum of squared differences after
206 combining two clusters into a single cluster. The shortest of these links (minimum increase in the sum of squared
207 differences) that remains at any step causes the fusion of the two clusters whose elements are involved.

208 A difficulty associated with cluster analysis is determining the most appropriate number of clusters given the
209 data because no a priori optimal number of clusters exists. Clusters resulting from alternative choices can be evaluated
210 through internal cluster validity indices (CVI); there are a variety of CVIs, most of which combine within cluster
211 cohesion (intra-cluster variance) or between cluster separation (inter-cluster variance) to compute a quality measure.
212 There is no universally best CVI (Arbelaitz et al. 2013), therefore we calculated a suite of five CVIs, including the
213 Silhouette, Gap, Davies–Bouldin, Calinski–Harabasz, and generalized Dunn indices, using the NbClust R package
214 (Charrad et al. 2014). A final number of clusters was determined by a majority rules approach based on the optimal
215 number of clusters suggested by each index (Table S2).

216 To determine whether clusters assignment were stable, or preserved under a perturbed dataset similar to the
217 original and therefore likely reflective of real differences, we conducted a bootstrapping approach where sites were
218 sampled with replacement and then AHC was performed on the resampled data using the fpc R package (Hennig
219 2020). For each bootstrapped cluster, we assessed the similarity between each new cluster and the most similar original
220 cluster with the Jaccard index. The Jaccard coefficient ranges from 0 to 1. Clusters with a coefficient larger than 0.75
221 were considered stable and clusters with a mean Jaccard coefficient of less than 0.5 were considered unstable and may
222 not reflect a true pattern in the data (Maheu et al. 2016, Savoy et al. 2019). We repeated the bootstrapping procedure
223 10,000 times; the mean Jaccard coefficient for each cluster is reported in Table 4.

224 **2.3.4 Identification of environmental drivers in thermal sensitivity**

225 We used classification and regression trees (CART; Breiman et al. 1984) to investigate the relative importance of
226 climatic, landscape, and physical drainage basin attributes for predicting each site's membership to a thermal
227 sensitivity cluster. CART is typically used to attempt to predict membership to clusters using environmental attributes,
228 and it allows the modelling of nonlinear relationships among mixed variable types and facilitates the examination of
229 intercorrelated variables in the final model (De'ath and Fabricius 2000, Olden et al. 2008). We took an exploratory
230 approach to this analysis due to our relatively small sample size ($N_{\text{Snoqualmie}} = 42$, $N_{\text{Wenatchee}} = 31$), which limited our
231 ability to conduct statistical tests. Therefore, we calculated variable relative importance, defined as the sum of squared
232 improvements at all splits determined by the predictor. These values are scaled to sum to 100 (rounded). We used the
233 R package rpart (Therneau and Atkinson 2019) for implementing the CART model. Covariates examined are described
234 in Table 1.

235 **3 Results**

236 **3.1 General patterns in temperature, precipitation, and thermal sensitivity**

237 This analysis included data from seven hydrologic years, each with differing temperature and precipitation patterns.
238 Generally, the years spanned by our dataset were warmer than the historical average, with wetter than average winter
239 and fall months and drier spring and summer months (Figure S1). The long-term average annual precipitation was
240 1874 mm (939 mm) for the western (eastern) Cascades time series. For the western (eastern) Cascades, all years (2015-
241 2021) have average annual temperatures higher than the long-term average of 8.6 °C (3 °C), although individual
242 seasons were slightly cooler than average. The year 2015 stood out as a year with an exceptionally warm winter, low
243 snowpack, and dry spring. Temperature and precipitation patterns in the western and eastern Cascades were generally
244 similar, however, precipitation anomalies were typically smaller in the eastern Cascades due to the overall lower
245 precipitation in this region (Figure 2; Figure S1).

246 Summary metrics describing air-water temperature relationships exhibited substantial variation across time
247 (season and year) and space. Across all season-year combinations, thermal sensitivities ranged from 0.05 to 0.97
248 (mean = 0.54) in the Snoqualmie basin and from 0.06 to 0.74 (mean = 0.42) in the Wenatchee basin (Table 2). Seasonal
249 distributions of thermal sensitivities differed. For example, fall thermal sensitivities were relatively homogeneous,
250 with 90% of values falling between 0.47 and 0.70, whereas spring and summer thermal sensitivities exhibited a broader

251 range of values, with 90% of values falling between 0.30 and 0.84 in spring and 0.25 and 0.78 in summer. Air
252 temperature was generally a good predictor of water temperature, as evidenced by R^2 values that ranged from 0.20 to
253 0.99 (mean = 0.88) in the Snoqualmie basin and from 0.08 to 0.98 (mean = 0.85) in the Wenatchee basin (Table 2).

254 Overall, weak and inconsistent patterns emerge in summer between thermal sensitivity and landscape and
255 climate variables (Figure 3; Table 3). For climate variables, only SWE appeared to have a linear relationship with
256 thermal sensitivity (Figure 3). The relationship between SWE and thermal sensitivity was negative and non-linear,
257 displaying a wedge-shaped pattern wherein large snowmelt events did not reduce thermal sensitivities below 0.25
258 (Figure 3). For landscape variables, correlation coefficients were overall small ($|\rho| < 0.3$), indicating weak to non-
259 existent linear relationships between landscape covariates and observed thermal sensitivity (Table 3). A weakly
260 negative relationship between thermal sensitivity and distance upstream was observed for both basins. Percent riparian
261 forests and thermal sensitivity showed no relationship for either basin. The relationship between hydraulic
262 conductivity and thermal sensitivity was weakly positive and parabolic in the Snoqualmie basin.

263 **3.2 Patterns of clustering for water temperatures, air temperatures, and thermal sensitivities**

264 Time-varying thermal sensitivities displayed periods of both high and low values within a season, which was not
265 necessarily represented when looking only at seasonal summary metrics (Figure 4 and Figure 5). Thermal sensitivity
266 varied alongside water and air temperature within the Snoqualmie and Wenatchee basins. Generally, thermal
267 sensitivity rose sharply in late spring, was highest in late summer, declined slowly throughout the fall, and remained
268 depressed through winter and early spring.

269 Spatially weighted AHC yielded four clusters for thermal sensitivity, with a cluster validity index (CVI)
270 range of 2-4, and two clusters each for air (CVI range of 2-5) and water (CVI range of 2-4) temperature in the
271 Snoqualmie basin, and five clusters for thermal sensitivity (CVI range 2-5) and two clusters each for air (CVI range
272 of 2-3) and water (CVI range of 2-5) temperature in the Wenatchee basin (Figure 4; Figure 5; Table S2). For both
273 basins, clusters of air and water temperature correspond closely with elevational gradients (Figure S4; Figure S5).
274 Higher elevation sites exhibited generally lower magnitudes but similar patterns in air and water temperatures (Table
275 4). For example, within both basins seasonal water temperatures were synchronized, with the cluster minimum and
276 maximum water temperatures occurring within a day of each other (Table 4). In the Snoqualmie basin, air temperature
277 clusters were stable, with a mean Jaccard index of 0.91 for high elevation sites (Cluster 2) and 0.73 for low elevation
278 sites (Cluster 1). Water temperature clusters were slightly less stable, with a mean Jaccard index of 0.65 for high

279 elevation sites (Cluster 2) and 0.89 for low elevation sites (Cluster 1). Air and water temperature clusters in the
280 Wenatchee basin were more stable than the Snoqualmie clusters. In the Wenatchee basin, air (water) temperature
281 clusters had a mean Jaccard index of 0.85 (0.86) for high elevation sites (Cluster 2) and 0.95 (0.73) for low elevation
282 sites (Cluster 1).

283 Clustering patterns for thermal sensitivity were more complex and less stable than air and water temperature
284 clusters, particularly for the Snoqualmie basin (Figure 4; Figure 5; Table 4). In the Snoqualmie basin, Cluster 1
285 consisted primarily of low elevation tributaries that exhibited stable thermal sensitivities throughout the year,
286 producing a cluster-average range of only 0.15 (Figure 4; Table 4). Cluster 2 was small (n=5), and the distribution of
287 sites within this cluster included three mainstem sites and two high elevation tributaries. Despite the large geographic
288 distances separating sites, this cluster was highly stable with a mean Jaccard index of 0.88. Cluster 2 was characterized
289 by a mean thermal sensitivity of 0.52 and the highest annual variability, with a cluster-average range of 0.45. Cluster
290 3 was large (n=15) and contained sites located within the upper regions of the Snoqualmie River. Cluster 3 had the
291 lowest mean thermal sensitivity (mean=0.40). Lastly, Cluster 4 exhibited the lowest stability of any cluster in the
292 Snoqualmie basin, with a mean Jaccard index of 0.55. Sites in this cluster were mainly situated on the mainstem
293 Snoqualmie and its major tributaries. This cluster was distinguished by the highest mean thermal sensitivity
294 (mean=0.65). In the Wenatchee basin, all five thermal sensitivity clusters were relatively stable. Clusters 1, 4, and 5
295 demonstrated similar seasonal patterns in thermal sensitivities, with minimum values occurring in late Spring (water
296 days 216, 207, 214) and maximum values occurring in late summer (water days 324, 331, 330). These clusters also
297 showed moderate to high stability (mean Jaccard indices of 0.79, 0.86, and 0.79). Cluster 3 exhibited the highest mean
298 thermal sensitivity (mean=0.40) and encompassed primarily low elevation tributaries (Peshastin and Mission Creek;
299 Figure S5). Cluster 2 was unique in that it consisted of a single site (Chumstick Creek) that was nearly always assigned
300 to a unique cluster when included in the bootstrapping procedure. The thermal sensitivity for this site was low
301 (mean=0.29) and virtually flat throughout the year (range = 0.07).

302 CART analysis indicated that basin topography and hydrogeology were the principal discriminators of
303 thermal sensitivity clusters. The top predictors of cluster membership (i.e., predictors with a greater than 10% increase
304 in mean standard error if removed from the model) were MWE and baseflow index in the Wenatchee basin and
305 watershed slope, MWE, and soil depth in the Snoqualmie basin (Figure 6). Variable importance distributions differed
306 between the Wenatchee and Snoqualmie basins, although in both basins several covariates had similar relative

307 importance values. Covariate distributions also varied across clusters within a basin. In the Snoqualmie basin, Cluster
308 1 sites were generally below a MWE of 600 meters, whereas Cluster 3 sites were generally mid-sized and high
309 elevation with a low baseflow index. In the Wenatchee basin, Cluster 1, 4, and 5 sites were predominately located at
310 high elevations with steep slopes. Cluster 4 sites exhibited a large proportion of precipitation falling as rain. Sites in
311 Clusters 2 and 3 were generally low elevation sites with a high baseflow index and soil depth.

312 **4 Discussion**

313 Thermal sensitivity varies throughout the year and reflects hydrologic conditions at a given time and place within a
314 watershed; therefore, it should not be conceptualized as a static value. Although summary metrics of thermal
315 sensitivity, such as average values over the summer, can still prove useful and informative, it is essential to
316 acknowledge the non-stationarity of the relationship between air and water temperature to obtain an accurate
317 understanding of how river temperature responds to changing conditions. Underlying geology and climate are
318 important controls on thermal sensitivity across two Pacific Northwest river basins and reflect aspects of river
319 dynamics not redundant with water and air temperature. Overall, this study provides a framework for using thermal
320 sensitivity regimes to improve understanding of factors contributing to stream temperatures and will enable managers
321 to target mitigation and adaptation activities to work best with local conditions within a watershed.

322 **4.1 Patterns of thermal sensitivity clustering**

323 Our analysis of stream air and water temperatures supports the presence of distinct thermal sensitivity regimes,
324 providing an organizing framework for river research and management by identifying sites with similarities across the
325 network. We found that thermal sensitivity regimes reflected non-redundant aspects of river dynamics relative to air
326 and water temperature alone. Air temperature and water temperature clusters closely corresponded to one another and
327 were almost entirely determined by elevation of the temperature loggers, whereas thermal sensitivity clusters showed
328 more variability in annual patterns and were intermixed spatially (Figure 4; Figure 5). Previous studies within the
329 Pacific Northwest found that, generally, colder streams are less sensitive to air temperature fluctuations than warmer
330 streams (Luce et al. 2014). Air and water clustering results are consistent with previous studies that observed broad
331 temporal correspondence of air and river temperature dynamics with differing magnitudes of response (Bower et al.
332 2004, Chu et al. 2010, Garner et al. 2014, Isaak et al. 2018a). More locally, Isaak et al. (2020) found that across

333 western rivers, much of the information in stream temperature records could be summarized by a relatively limited
334 number of distinct regime components primarily driven by differences in elevation and latitude.

335 Viewing thermal sensitivity as a continuous parameter adds novel insights to our understanding of river basin
336 functioning. Studies have highlighted the importance of annual shifts in the processes that drive heat budgets as well
337 as the non-stationarity of the resulting statistical relationships (Arismendi et al. 2014, Boyer et al. 2021). Our clustering
338 analysis overcomes these issues by using a varying coefficient model that treats thermal sensitivity as a continuous
339 function through time, rather than a series of discrete summary metrics, and allows clustering based on the entirety of
340 average annual patterns. The observed complexity in thermal sensitivity response hints at the diversity of physical
341 processes controlling stream temperature response and the large, clear shifts in thermal sensitivity magnitude across
342 the year calls into question the common practice of summarizing a river's sensitivity as a static value. The ability to
343 directly observe shifts in the air-water temperature relationships also opens the possibility of using thermal sensitivity
344 as a diagnostic tool to examine gradual changes in the importance of drivers of water temperature, such as dynamic
345 changes in riparian shading or snowmelt.

346 **4.2 Climate controls on thermal sensitivity**

347 Seasonal variability of thermal sensitivity metrics was evident for our basins. Within both the Snoqualmie and
348 Wenatchee basins, winter thermal sensitivities were low and varied strongly with MWE (Figure 1). Observed low
349 thermal sensitivities in winter were likely due to the non-linear relationship between air and stream temperature at
350 cold temperatures when air temperatures can dip below the water temperature-freezing limit (Mohseni et al. 1998,
351 1999). Air temperature covaries strongly with elevation in Pacific Northwest basins, and sites that are high in the
352 watershed will experience a greater number of sub-freezing days, and therefore greater decoupling between air and
353 water temperatures. Fall thermal sensitivities were relatively homogeneous whereas spring and summer thermal
354 sensitivities exhibited a broader range of values. We expect thermal sensitivities to be similar during periods of heavy
355 precipitation, when water sources with thermal characteristics distinct from air temperature, such as groundwater and
356 snowmelt, contribute relatively less flow. The greater variability of responses in spring and summer indicates that the
357 processes controlling river temperatures are more diverse than in fall or winter (Hrachowitz et al. 2010).

358 Snowmelt likely contributed to observed differences in thermal sensitivity across sites in spring and early
359 summer. For summary metrics, the relationship between snowmelt and spring thermal sensitivity formed a wedge-
360 shaped pattern, wherein sites with limited snowmelt displayed both high and low thermal sensitivity, but sites with

361 extensive snowmelt always display low thermal sensitivity (Figure 3). For the clustering analysis, although the
362 proportion of precipitation falling as snow showed limited variable importance, MWE and slope covaried closely with
363 snow accumulation and were among the most important predictors of cluster membership, perhaps masking a
364 statistical signal of snowfall (Figure 6). In both the Snoqualmie and Wenatchee basins, clusters with higher elevation,
365 steeper slope, and greater snowmelt within the catchment had thermal regimes that were less sensitive to changes in
366 air temperature during spring and early summer. Importantly, snowmelt buffering, the process wherein snowmelt-
367 influenced streams have lower thermal sensitivity due to a direct input of cold water and a corresponding increase in
368 flow rates and water depths (van Vliet et al. 2011, Siegel et al. 2022), diminishes throughout the summer. By late
369 summer, high elevation, snowmelt influenced sites were often more sensitive to air temperatures than their low
370 elevation counterparts (Figure 4; Figure 5). Sites within Cluster 4 in the Wenatchee basin were an exception to this
371 pattern and maintained summer thermal sensitivities that were substantially depressed relative to adjacent locations
372 (e.g., Clusters 1 and 5). This is likely due to glacial inputs within these catchments, and points to the importance of
373 high elevation glacial and late-summer snowpack melt as a significant source of summer baseflow and control on
374 water temperatures during the months of greatest heating within these watersheds.

375 Numerous studies have examined the buffering impact of snowmelt on water temperature due to advective
376 flux from cooler meltwater entering the river. Studies in Alaskan rivers found a linear, negative relationship between
377 summer thermal sensitivity and snowmelt (Lisi et al. 2015, Cline et al. 2020) and a recent study in the Snoqualmie
378 basin found that snowmelt can reduce basin-wide peak summer temperatures, particularly at high elevation tributaries,
379 and the thermal impacts of melt water can persist through the summer (Yan et al. 2021). Our results suggest that
380 snowpack offers substantial buffering to changes in air temperature across mountain river basins, but that the largest
381 impacts are localized across space and time. Climate change is expected to shift snowmelt earlier and reduce snow
382 water resources (Barnett et al. 2005, Musselman et al. 2021). The loss of snow may result in warming in snow-
383 influenced systems and the subsequent homogenization of thermal conditions across basins (Winfrey et al. 2018).
384 Homogenization of thermal conditions likely leads to important changes in ecological functions and ecosystem
385 services supported by lost thermal heterogeneity, such as a loss of cold-water patches for Pacific salmon (Brennan et
386 al. 2019).

387 **4.3 Geologic controls on thermal sensitivity**

388 Geologic characteristics shaped the relationship between air and water temperatures across the Wenatchee and
389 Snoqualmie basins. The inclusion of baseflow index, hydraulic conductivity, and soil depth in determining cluster
390 membership (Figure 6) implies the importance, and detectability, of groundwater as a key mediator of thermal
391 sensitivity regimes in Pacific Northwest basins. Clusters with high baseflow index, hydraulic conductivity, and soil
392 depth values generally had lower summer and less variable thermal sensitivities (Figure 4; Figure 5; Figure 6),
393 implying greater groundwater influence (Kelleher et al. 2012). Interestingly, despite the clear importance of
394 groundwater metrics in the clustering analysis, results from summary metric exploratory analysis were mixed and, in
395 the Snoqualmie basin, did not align with expectations of a negative relationship between thermal sensitivity and
396 groundwater influence (Table 3). Although it is possible to infer broad patterns in surface-groundwater connectivity
397 using datasets of interpolated hydrogeologic properties (i.e., hydraulic conductivity, soil depth) or water source (i.e.,
398 baseflow index), individual hydrogeologic metrics often have substantial uncertainty, do not covary perfectly, and
399 may be particularly unconstrained for mountain headwater streams (Wolock et al. 2004, Patton et al. 2018, Briggs et
400 al. 2022). Additionally, the influence of these processes can be localized and variable across space (Johnson et al.
401 2017) and substantially impacted by human modification. The ability to use thermal sensitivity as an empirical
402 measure of groundwater influence, therefore, shows great promise for understanding catchment processes and
403 informing management and restoration actions at ecologically relevant scales (Snyder et al. 2015).

404 An investigation of the underlying geology across the Snoqualmie and Wenatchee basins supports our
405 conclusion that low thermal sensitivities are indicative of groundwater inputs. The lowland portion of the Snoqualmie
406 watershed contains a deep, permeable, productive glacial aquifer that is presumed to be the source of summer baseflow
407 to much of the river (Bethel 2004, McGill et al. 2021, Turney et al. 1995). Glacial and interglacial deposits in the
408 valley contain several geohydrologic units with differing aquifer potential (Bethel 2004); however, most deposits can
409 form small but useable aquifers that could be helping to sustain baseflow in summer months (Turney et al. 1995,
410 Soulsby et al. 2004, Blumstock et al. 2015). Soil depth, hydraulic conductivity, and baseflow index were
411 correspondingly high in streams that overlay the lower portion of the watershed (Figure 6). Thermal sensitivities
412 reflected this pattern, wherein generally sites draining low elevation tributaries (Cluster 1) had relatively constant
413 thermal sensitivities throughout the year (Figure 4). Conversely, the upper portion of the Snoqualmie basin is covered
414 by thin soil over impermeable bedrock lacking extensive fracture networks, meaning that rain and snowmelt are not

415 retained in the mountains but are rapidly transmitted to the stream system (Debose and Klungland 1964, Nelson 1971,
416 Goldin 1973, 1992). Sites with catchments predominantly within this upland area tended to belong to Clusters 2 and
417 3 and displayed high summer thermal sensitivities, perhaps indicating limited groundwater influence.

418 In the Wenatchee basin, two major aquifers exist: an aquifer within the sedimentary bedrock of the central
419 and lowland areas and an overlying unconsolidated alluvial and outwash aquifer located primarily in river valley
420 bottoms across the basin (Montgomery Water Group 2003). The bedrock aquifer consists of sandstones and shales,
421 which tend to have moderately low permeability. Folding and faulting have caused the shale to break up or fracture
422 and groundwater moves preferentially within these zones of higher secondary permeability. The alluvial and outwash
423 aquifers, on the other hand, exhibit relatively high permeability where groundwater can move easily and are considered
424 the primary groundwater source (Wildrick 1979, Montgomery Water Group 2003). Cluster 2 in the Wenatchee basin,
425 consisting of a single site located at the mouth of Chumstick Creek (Figure S5), stands out for having a unique, nearly
426 flat thermal sensitivity compared to patterns at other sites (Figure 5). Covariate distributions for the clustering results
427 showed that Chumstick Creek has a relatively high hydraulic conductivity and baseflow index (Figure 6; Figure S7).
428 A transition from low to high permeability glacial material occurs near the mouth of Chumstick Creek (Montgomery
429 Water Group 2003), and it is possible that substantial groundwater discharge occurs near this discontinuity (Neff et
430 al. 2019). Similarly, sites within Cluster 3 showed low variability in thermal sensitivity and had high soil depth and
431 baseflow index values. Streams within this cluster are situated on top of predominantly sandstone bedrock (Frizzell
432 1979, Gendaszek et al. 2014).

433 Overall, the importance of groundwater is consistent with previous studies, which find that thermal sensitivity
434 decreased with increasing groundwater contribution (O'Driscoll and DeWalle 2006, Chang and Psaris 2013, Beaufort
435 et al. 2020, Georges et al. 2021). The degree to which groundwater decouples trends in stream and air temperature
436 depends on stream volume, the rate of groundwater inflow, and the depth of groundwater source. Although not
437 examined in this study, aquifer source and groundwater depth likely influence thermal sensitivity estimates, with
438 runoff sourced from deep groundwater being less variable and less sensitive in comparison to groundwater sourced
439 from shallow sub-surface flows (Tague et al. 2007, Johnson et al. 2021, Hare et al. 2021). Shallow groundwater
440 temperatures are already responding to climate change (Menberg et al. 2014). As warming continues, the summer
441 cooling capacity of groundwater may be reduced, limiting the availability of cold-water refugia patches sourced by
442 groundwater (Brewer 2013, Briggs et al. 2013).

443 **4.4 Landscape controls on thermal sensitivity**

444 Variable relationships between thermal sensitivities and landscape covariates highlight complexities in stream thermal
445 regimes. For example, mean channel slope was an important predictor of cluster membership for both the Snoqualmie
446 and Wenatchee basins, but showed a weak-to-non-existent relationship with summer thermal sensitivity summary
447 metrics. Steeper channel slopes and greater stream velocities limit warming in streams by decreasing the time for
448 equilibration with local heating conditions (Donato 2002, Webb et al. 2008, Isaak et al. 2012) and topographic shading
449 associated with steep watersheds can suppresses stream temperature by reducing exposure to solar radiation (Webb
450 and Zhang 1997). In the Wenatchee basin, the Cluster 3 site, Chumstick Creek, drains a steep canyon. This may
451 contribute to observed low, stable thermal sensitivities throughout the year. Additionally, watershed size and distance
452 upstream covary closely and displayed relatively consistent relationships with summer thermal sensitivity summary
453 metrics despite ranking moderately in variable importance. We expected thermal sensitivity to increase with river size;
454 groundwater influence should be more visible on smaller streams because the volume of water is small and the travel
455 time of the water from the source is short and not sufficient to equilibrate water temperature with the atmosphere
456 (Mohseni and Stefan 1999, Tague et al. 2007, Beaufort et al. 2016). Reduced sensitivity of headwater streams to air
457 temperature was observed in the Aberdeenshire Dee, Scotland (Hrachowitz et al. 2010), and River Danube, Austria
458 (Webb and Nobilis 2007), and small Pennsylvanian streams were shown to be less sensitive to changes in air
459 temperature than larger streams (Kelleher et al. 2012). However, Hilderbrand et al. (2014) found no relationship
460 between thermal sensitivity and watershed size in Maryland streams.

461 We expected landscape covariates to be important predictors of thermal sensitivity regimes, however, these
462 covariates were of limited importance and showed no relationship with summary metrics (Table 3; Figure 6). Several
463 factors may account for this. Inherent covariation in river basins can hinder statistical efforts to identify mechanistic
464 links between landscape gradients and features of aquatic ecosystems (Lucero et al. 2011); land cover characteristics
465 may have a small impact that went undetected due to noisy observations or limited variability within our study region.
466 It is also possible that land cover metrics may not adequately describe the intended process. For example, the relative
467 unimportance of riparian shading may be due in part to our metric of shade, which was limited to riparian forest cover
468 and ignored topographic shading and vegetation height. Lastly, human modifications to the river that are not captured
469 by land cover statistics, such as channelization or the presence of dams and reservoirs, may alter thermal sensitivity
470 and obscure natural gradients. For example, areas of the river that are degraded and subsequently disconnected from

471 their floodplain may have artificially high thermal sensitivities, and the release of water from dams and reservoirs has
472 the potential to either warm or cool downstream temperatures, depending on dynamics of where and how impounded
473 water is released (Ahmad et al. 2021, Cheng et al. 2022). Future research could include covariates sinuosity or variance
474 of thalweg depth to better capture these effects. Untangling exact controls will require additional research.

475 **4.5 Caveats and limitations**

476 Due to the realities of data collection in dynamic systems, time series of both air and water temperature used in this
477 analysis have periods of missing values that span weeks to months. Classical clustering techniques require complete
478 datasets, limiting analyses to time series without gaps. To overcome this issue, we calculated a single representative
479 time series at each site that captures the typical range and timing of thermal sensitivity. Alternative options for dealing
480 with missing values include removing data points that do not cover the target time period or imputing missing values
481 by means of statistical procedures or summary metrics (e.g., Savoy et al. 2019, Beaufort et al. 2020). However, we
482 chose not to use these approaches in our study due to the long and inconsistent periods of missing values across sites.
483 We acknowledge that interannual variability in precipitation and temperature impacts river thermal sensitivity, and
484 average time series calculated from differing years may exhibit differences in shape and timing for reasons outside of
485 inherent characteristics (Appendix A). Future studies could use novel clustering methods capable of dealing with
486 sparse datasets, which would provide more detailed information on clusters generated from time periods with robust
487 values versus data scarcity (Carro-Calvo et al. 2021). Alternatively, recent advances in space-time imputation for
488 river basins may prove a fruitful direction (Li et al. 2017).

489 Our calculation of time-varying thermal sensitivities also necessitated decisions regarding what features of the
490 time series to preserve. Selection of the bandwidth parameter and kernel function for the time varying model will
491 impact estimation of thermal sensitivity and intercept. Generally, with larger bandwidth estimates or averaging periods
492 (e.g., daily, weekly, monthly), intercept estimates increase and thermal sensitivity estimates decrease. Decisions of
493 this nature should be approached carefully and with a clear question in mind. For this study, we were interested in
494 seasonal to annual patterns in thermal sensitivity, and thus chose a bandwidth of 0.2, resulting in a smooth seasonal
495 time series. Previous studies have also used regression splines to estimate the time varying relationship between air
496 and water temperatures (Haggarty et al. 2015). This approach smooths data and can account for missing data but may
497 not preserve small-scale features of interest. We chose to use absolute values of our thermal sensitivity time series, as

498 we cared about differences in mean thermal sensitivity as well as correlated variability. Future work could normalize
499 thermal sensitivity time series first to examine only patterns.

500 **4.6 Implications for management and future directions**

501 Classifying rivers based on thermal sensitivity could be a powerful tool when planning for global change. Our results
502 show that annual patterns in thermal sensitivity are diverse and mediated by underlying geology and climate across
503 two Pacific Northwest river basins. Climate change is decreasing snowpack in the region, resulting in earlier runoff
504 and extended summer baseflow (Elsner et al. 2010, Wu et al. 2012), and may decrease groundwater discharge
505 depending on sources and timing of recharge (Brooks et al. 2012, McGill et al. 2021). For many of our study sites,
506 thermal sensitivities were highest in late summer during the hottest, lowest flow portion of the year. Previous studies
507 have found that the impact of fluctuations in discharge generally increases during dry, warm periods, when rivers have
508 a lower thermal capacity and are more sensitive to atmospheric warming (van Vliet et al. 2013). High thermal
509 sensitivity in late summer and in high elevation streams, which are typically thought to be climate refuges, is therefore
510 troubling for the conservation of native coldwater species such as Pacific salmon (Mantua et al. 2010; Isaak et al.
511 2016). Climate change will likely decrease juvenile rearing and spawning habitat quantity and quality, although it is
512 important to note that streams with high thermal sensitivity may still provide adequate habitat in select portions of the
513 year if stress-related thresholds are not exceeded (Armstrong et al. 2021).

514 Examining thermal sensitivity regimes improves understanding of factors contributing to stream
515 temperatures and may enable managers to target mitigation and adaptation activities to work best with local conditions,
516 thus maximizing benefits given limited resources. For example, given the importance of subsurface geology within
517 the Wenatchee and Snoqualmie basins, targeted actions to restore floodplain functions that recharge aquifers through
518 actions such as placing engineered logjams or reintroducing beavers could be prioritized (Abbe and Brooks 2013,
519 Pollock et al. 2014, Jordan and Fairfax 2022). Additionally, identification of particularly insensitive portions of the
520 river could help to better constrain areas where coldwater patches exist that may be used as refuges for coldwater fish
521 (Snyder et al. 2020). This process-based approach will be particularly important as non-stationary relationships caused
522 by climate change make it unreliable to use past regressions built under historical climate conditions (Boyer et al.
523 2021). Furthermore, as longer, more spatially extensive air and water temperature time series become available (Isaak
524 et al. 2017), we can begin to ask questions about 1) the spatial extent of different thermal sensitivity regimes, 2) how
525 interannual variability shifts with climate conditions and geographic context, and 3) detect changes in the external

526 drivers of thermal sensitivities. Such insights will improve our understanding of river ecosystems while offering a
527 suite of new tools for monitoring the impact of management decisions and climate change.

528 **Acknowledgements**

529 We thank Amy Marsha, Roxana Rautu, Akida Ferguson, Shannon Claeson and the many volunteers for help collecting
530 air and water temperature data, and Gordon Holtgrieve, Mark Scheuerell, and Christopher Jordan for suggestions that
531 improved the manuscript. This material is based upon work supported by the National Science Foundation Graduate
532 Research Fellowship under Grant No. DGE-1762114. Any opinion, findings, and conclusions or recommendations
533 expressed in this material are those of the authors and do not necessarily reflect the views of the National Science
534 Foundation.

535 **Author Contributions and Data Availability**

536 All authors conceptualized the study and retrieved the data. LMM analyzed the data and prepared the manuscript with
537 the assistance of EAS and AHF. The data that supports the findings of this study are available at
538 <https://github.com/lmcgill/AirWaterCorr/tree/master/data> and can be visualized at
539 https://lmcgill.shinyapps.io/TimeVarying_AWC/. The authors have no competing interests to declare.

540 **References**

- 541 Abbe, T., and A. Brooks. 2013. Geomorphic, Engineering, and Ecological Considerations when Using Wood in River
542 Restoration. Pages 419–451 in A. Simon, S. J. Bennett, and J. M. Castro, editors. Geophysical Monograph
543 Series. American Geophysical Union, Washington, D. C.
- 544 Ahmad, S. K., F. Hossain, G. W. Holtgrieve, T. Pavelsky, and S. Galelli. 2021. Predicting the Likely Thermal Impact
545 of Current and Future Dams Around the World. *Earth's Future* 9.
- 546 Arbelaitz, O., I. Gurrutxaga, J. Muguerza, J. M. Pérez, and I. Perona. 2013. An extensive comparative study of cluster
547 validity indices. *Pattern Recognition* 46:243–256.
- 548 Arismendi, I., M. Safeeq, J. B. Dunham, and S. L. Johnson. 2014. Can air temperature be used to project influences
549 of climate change on stream temperature? *Environmental Research Letters* 9:084015.
- 550 Armstrong, J. B., A. H. Fullerton, C. E. Jordan, J. L. Ebersole, J. R. Bellmore, I. Arismendi, B. E. Penaluna, and G.
551 H. Reeves. 2021. The importance of warm habitat to the growth regime of cold-water fishes. *Nature Climate
552 Change* 11:354–361.
- 553 Barnett, T. P., J. C. Adam, and D. P. Lettenmaier. 2005. Potential impacts of a warming climate on water availability
554 in snow-dominated regions. *Nature* 438:303–309.
- 555 Beaufort, A., F. Moatar, F. Curie, A. Ducharne, V. Bustillo, and D. Thiéry. 2016. River Temperature Modelling by
556 Strahler Order at the Regional Scale in the Loire River Basin, France: River Temperature Modelling by
557 Strahler Order. *River Research and Applications* 32:597–609.
- 558 Beaufort, A., F. Moatar, E. Sauquet, P. Loicq, and D. M. Hannah. 2020. Influence of landscape and hydrological
559 factors on stream–air temperature relationships at regional scale. *Hydrological Processes* 34:583–597.
- 560 van Beek, L. P. H., T. Eikelboom, M. T. H. Vliet, and M. F. P. Bierkens. 2012. A physically based model of global
561 freshwater surface temperature. *Water Resources Research* 48:2012WR011819.
- 562 Benyahya, L., D. Caissie, N. El-Jabi, and M. G. Satish. 2010. Comparison of microclimate vs. remote meteorological
563 data and results applied to a water temperature model (Miramichi River, Canada). *Journal of Hydrology*
564 380:247–259.
- 565 Benyahya, L., D. Caissie, A. St-Hilaire, T. B. M. J. Ouarda, and B. Bobée. 2007. A Review of Statistical Water
566 Temperature Models. *Canadian Water Resources Journal* 32:179–192.

567 Bethel, J. 2004. An overview of the geology and geomorphology of the Snoqualmie River watershed. King County
568 Water and Land Resources Division, Snoqualmie Watershed Team.

569 Blumstock, M., D. Tetzlaff, I. A. Malcolm, G. Nuetzmann, and C. Soulsby. 2015. Baseflow dynamics: Multi-tracer
570 surveys to assess variable groundwater contributions to montane streams under low flows. *Journal of*
571 *Hydrology* 527:1021–1033.

572 Bogan, T., O. Mohseni, and H. G. Stefan. 2003. Stream temperature-equilibrium temperature relationship. *Water*
573 *Resources Research* 39.

574 Bower, D., D. M. Hannah, and G. R. McGregor. 2004. Techniques for assessing the climatic sensitivity of river flow
575 regimes. *Hydrological Processes* 18:2515–2543.

576 Boyer, C., A. St-Hilaire, and N. E. Bergeron. 2021. Defining river thermal sensitivity as a function of climate. *River*
577 *Research and Applications* 37:1548–1561.

578 Breiman, L., J. H. Friedman, R. A. Olshen, and C. J. Stone. 1984. *Classification And Regression Trees*. First edition.
579 Routledge.

580 Brennan, S. R., D. E. Schindler, T. J. Cline, T. E. Walsworth, G. Buck, and D. P. Fernandez. 2019. Shifting habitat
581 mosaics and fish production across river basins. *Science* 364:783–786.

582 Brewer, S. K. 2013. GROUNDWATER INFLUENCES ON THE DISTRIBUTION AND ABUNDANCE OF
583 RIVERINE SMALLMOUTH BASS, *MICROPTERUS DOLOMIEU* , IN PASTURE LANDSCAPES OF
584 THE MIDWESTERN USA. *River Research and Applications* 29:269–278.

585 Briggs, M. A., P. Goodling, Z. C. Johnson, K. M. Rogers, N. P. Hitt, J. B. Fair, and C. D. Snyder. 2022. Bedrock depth
586 influences spatial patterns of summer baseflow, temperature, and flow disconnection for mountainous
587 headwater streams. preprint, *Catchment hydrology/Instruments and observation techniques*.

588 Briggs, M. A., Z. C. Johnson, C. D. Snyder, N. P. Hitt, B. L. Kurylyk, L. Lautz, D. J. Irvine, S. T. Hurley, and J. W.
589 Lane. 2018. Inferring watershed hydraulics and cold-water habitat persistence using multi-year air and stream
590 temperature signals. *Science of The Total Environment* 636:1117–1127.

591 Briggs, M. A., E. B. Voytek, F. D. Day-Lewis, D. O. Rosenberry, and J. W. Lane. 2013. Understanding Water Column
592 and Streambed Thermal Refugia for Endangered Mussels in the Delaware River. *Environmental Science &*
593 *Technology* 47:11423–11431.

594 Brooks, J. R., P. J. Wigington, D. L. Phillips, R. Comeleo, and R. Coulombe. 2012. Willamette River Basin surface
595 water isoscape ($\delta^{18}\text{O}$ and $\delta^2\text{H}$): temporal changes of source water within the river. *Ecosphere* 3:art39.

596 Caissie, D. 2006. The thermal regime of rivers: a review. *Freshwater Biology* 51:1389–1406.

597 Carro-Calvo, L., F. Jaume-Santero, R. García-Herrera, and S. Salcedo-Sanz. 2021. k-Gaps: a novel technique for
598 clustering incomplete climatological time series. *Theoretical and Applied Climatology* 143:447–460.

599 Casas, I., and R. Fernandez-Casal. 2019. tvReg: Time-varying Coefficient Linear Regression for Single and Multi-
600 Equations in R. *SSRN Electronic Journal*.

601 Casas, I., and R. Fernandez-Casal. 2021. tvReg: Time-Varying Coefficients Linear Regression for Single and Multi-
602 Equations.

603 Chang, H., and M. Psaris. 2013. Local landscape predictors of maximum stream temperature and thermal sensitivity
604 in the Columbia River Basin, USA. *Science of The Total Environment* 461–462:587–600.

605 Charrad, M., N. Ghazzali, V. Boiteau, and A. Niknafs. 2014. NbClust: An R Package for Determining the Relevant
606 Number of Clusters in a Data Set. *Journal of Statistical Software* 61:1–36.

607 Cheng, Y., B. Nijssen, G. W. Holtgrieve, and J. D. Olden. 2022. Modeling the freshwater ecological response to
608 changes in flow and thermal regimes influenced by reservoir dynamics. *Journal of Hydrology* 608:127591.

609 Chu, C., N. E. Jones, and L. Allin. 2010. Linking the thermal regimes of streams in the Great Lakes Basin, Ontario,
610 to landscape and climate variables: THERMAL REGIMES IN ONTARIO STREAMS. *River Research and*
611 *Applications* 26:221–241.

612 Cline, T. J., D. E. Schindler, T. E. Walsworth, D. W. French, and P. J. Lisi. 2020. Low snowpack reduces thermal
613 response diversity among streams across a landscape. *Limnology and Oceanography Letters* 5:254–263.

614 Cressie, N. A. C. 1993. *Statistics for Spatial Data: Cressie/Statistics*. John Wiley & Sons, Inc., Hoboken, NJ, USA.

615 Daufresne, M., and P. Boët. 2007. Climate change impacts on structure and diversity of fish communities in rivers.
616 *Global Change Biology* 13:2467–2478.

617 De'ath, G., and K. E. Fabricius. 2000. Classification and regression trees: a powerful yet simple technique for
618 ecological data analysis. *Ecology* 81:3178–3192.

619 Debose, A., and M. W. Klungland. 1964. Soil survey of Snohomish County area. US Department of Agriculture, Soil
620 Conservation Service, Washington, D. C.

621 Donato, M. M. 2002. A statistical model for estimating stream temperatures in the Salmon and Clearwater River
622 basins, Central Idaho. Water Resources Investigations Report, U.S. Geological Survey, Washington, D. C.

623 Dugdale, S. J., D. M. Hannah, and I. A. Malcolm. 2017. River temperature modelling: A review of process-based
624 approaches and future directions. *Earth-Science Reviews* 175:97–113.

625 Elsner, M. M., L. Cuo, N. Voisin, J. S. Deems, A. F. Hamlet, J. A. Vano, K. E. B. Mickelson, S.-Y. Lee, and D. P.
626 Lettenmaier. 2010. Implications of 21st century climate change for the hydrology of Washington State.
627 *Climatic Change* 102:225–260.

628 Frizzell, V. A. 1979. Petrology and stratigraphy of Paleogene nonmarine sandstones, Cascade Range, Washington.
629 Open-File Report, U.S. Geological Survey.

630 Garner, G., D. M. Hannah, J. P. Sadler, and H. G. Orr. 2014. River temperature regimes of England and Wales: spatial
631 patterns, inter-annual variability and climatic sensitivity: RIVER TEMPERATURE REGIMES OF
632 ENGLAND AND WALES. *Hydrological Processes* 28:5583–5598.

633 Gendaszek, A. S., D. M. Ely, S. R. Hinkle, S. C. Kahle, and W. B. Welch. 2014. Hydrogeologic framework and
634 groundwater/surface-water interactions of the upper Yakima River Basin, Kittitas County, central
635 Washington. Scientific Investigations Report, U.S. Geological Survey.

636 Georges, B., A. Michez, H. Piegay, L. Huylenbroeck, P. Lejeune, and Y. Brostaux. 2021. Which environmental factors
637 control extreme thermal events in rivers? A multi-scale approach (Wallonia, Belgium). *PeerJ* 9:e12494.

638 Glose, A., L. K. Lautz, and E. A. Baker. 2017. Stream heat budget modeling with HFLUX: Model development,
639 evaluation, and applications across contrasting sites and seasons. *Environmental Modelling & Software*
640 92:213–228.

641 Goldin, A. 1973. Soil survey of King County area, Washington. US Department of Agriculture, Soil Conservation
642 Service, Washington, D. C.

643 Goldin, A. 1992. Soil survey of Whatcom County area, Washington. US Department of Agriculture, Soil Conservation
644 Service, Washington, D. C.

645 Haggarty, R. A., C. A. Miller, and E. M. Scott. 2015. Spatially weighted functional clustering of river network data.
646 *Journal of the Royal Statistical Society: Series C (Applied Statistics)* 64:491–506.

647 Hare, D. K., A. M. Helton, Z. C. Johnson, J. W. Lane, and M. A. Briggs. 2021. Continental-scale analysis of shallow
648 and deep groundwater contributions to streams. *Nature Communications* 12:1450.

649 Hennig, C. 2020. fpc: Flexible Procedures for Clustering.

650 Hilderbrand, R. H., M. T. Kashiwagi, and A. P. Prochaska. 2014. Regional and Local Scale Modeling of Stream
651 Temperatures and Spatio-Temporal Variation in Thermal Sensitivities. *Environmental Management* 54:14–
652 22.

653 Hoover, D. 1998. Nonparametric smoothing estimates of time-varying coefficient models with longitudinal data.
654 *Biometrika* 85:809–822.

655 Hrachowitz, M., C. Soulsby, C. Imholt, I. A. Malcolm, and D. Tetzlaff. 2010. Thermal regimes in a large upland
656 salmon river: a simple model to identify the influence of landscape controls and climate change on maximum
657 temperatures. *Hydrological Processes* 24:3374–3391.

658 Isaak, D. J., C. H. Luce, G. L. Chandler, D. L. Horan, and S. P. Wollrab. 2018a. Principal components of thermal
659 regimes in mountain river networks. *Hydrology and Earth System Sciences* 22:6225–6240.

660 Isaak, D. J., C. H. Luce, D. L. Horan, G. L. Chandler, S. P. Wollrab, W. B. Dubois, and D. E. Nagel. 2020. Thermal
661 Regimes of Perennial Rivers and Streams in the Western United States. *JAWRA Journal of the American
662 Water Resources Association* 56:842–867.

663 Isaak, D. J., C. H. Luce, D. L. Horan, G. L. Chandler, S. P. Wollrab, and D. E. Nagel. 2018b. Global Warming of
664 Salmon and Trout Rivers in the Northwestern U.S.: Road to Ruin or Path Through Purgatory? *Transactions
665 of the American Fisheries Society* 147:566–587.

666 Isaak, D. J., S. J. Wenger, E. E. Peterson, J. M. Ver Hoef, D. E. Nagel, C. H. Luce, S. W. Hostetler, J. B. Dunham, B.
667 B. Roper, S. P. Wollrab, G. L. Chandler, D. L. Horan, and S. Parkes-Payne. 2017. The NorWeST Summer
668 Stream Temperature Model and Scenarios for the Western U.S.: A Crowd-Sourced Database and New
669 Geospatial Tools Foster a User Community and Predict Broad Climate Warming of Rivers and Streams.
670 *Water Resources Research* 53:9181–9205.

671 Isaak, D. J., S. Wollrab, D. Horan, and G. Chandler. 2012. Climate change effects on stream and river temperatures
672 across the northwest U.S. from 1980–2009 and implications for salmonid fishes. *Climatic Change* 113:499–
673 524.

674 Isaak, D. J., M. K. Young, C. H. Luce, S. W. Hostetler, S. J. Wenger, E. E. Peterson, J. M. Ver Hoef, M. C. Groce, D.
675 L. Horan, and D. E. Nagel. 2016. Slow climate velocities of mountain streams portend their role as refugia
676 for cold-water biodiversity. *Proceedings of the National Academy of Sciences* 113:4374–4379.

677 Jackson, F. L., R. J. Fryer, D. M. Hannah, C. P. Millar, and I. A. Malcolm. 2018. A spatio-temporal statistical model
678 of maximum daily river temperatures to inform the management of Scotland's Atlantic salmon rivers under
679 climate change. *Science of The Total Environment* 612:1543–1558.

680 Johnson, S. L. 2003. Stream temperature: scaling of observations and issues for modelling. *Hydrological Processes*
681 17:497–499.

682 Johnson, Z. C., B. G. Johnson, M. A. Briggs, C. D. Snyder, N. P. Hitt, and W. D. Devine. 2021. Heed the data gap:
683 Guidelines for using incomplete datasets in annual stream temperature analyses. *Ecological Indicators*
684 122:107229.

685 Johnson, Z. C., C. D. Snyder, and N. P. Hitt. 2017. Landform features and seasonal precipitation predict shallow
686 groundwater influence on temperature in headwater streams. *Water Resources Research* 53:5788–5812.

687 Johnson, Z. C., J. J. Warwick, and R. Schumer. 2014. Factors affecting hyporheic and surface transient storage in a
688 western U.S. river. *Journal of Hydrology* 510:325–339.

689 Jordan, C. E., and E. Fairfax. 2022. Beaver: The North American freshwater climate action plan. *WIREs Water* 9.

690 Kelleher, C., T. Wagener, M. Gooseff, B. McGlynn, K. McGuire, and L. Marshall. 2012. Investigating controls on the
691 thermal sensitivity of Pennsylvania streams. *Hydrological Processes* 26:771–785.

692 Lance, G. N., and W. T. Williams. 1967. A general theory of classificatory sorting strategies: II. Clustering systems.
693 *The Computer Journal* 10:271–277.

694 Leach, J. A., and R. D. Moore. 2019. Empirical Stream Thermal Sensitivities May Underestimate Stream Temperature
695 Response to Climate Warming. *Water Resources Research* 55:5453–5467.

696 Li, H., X. Deng, C. A. Dolloff, and E. P. Smith. 2016. Bivariate functional data clustering: grouping streams based on
697 a varying coefficient model of the stream water and air temperature relationship. *Environmetrics* 27:15–26.

698 Li, H., X. Deng, D.-Y. Kim, and E. P. Smith. 2014. Modeling maximum daily temperature using a varying coefficient
699 regression model. *Water Resources Research* 50:3073–3087.

700 Li, H., X. Deng, and E. Smith. 2017. Missing data imputation for paired stream and air temperature sensor data:
701 Missing Data Imputation for Stream and Air Temperature. *Environmetrics* 28:e2426.

702 Lisi, P. J., D. E. Schindler, T. J. Cline, M. D. Scheuerell, and P. B. Walsh. 2015. Watershed geomorphology and
703 snowmelt control stream thermal sensitivity to air temperature. *Geophysical Research Letters* 42:3380–3388.

704 Luce, C., B. Staab, M. Kramer, S. Wenger, D. Isaak, and C. McConnell. 2014. Sensitivity of summer stream
705 temperatures to climate variability in the Pacific Northwest. *Water Resources Research* 50:3428–3443.

706 Maheu, A., N. L. Poff, and A. St-Hilaire. 2016. A Classification of Stream Water Temperature Regimes in the
707 Conterminous USA: Classification of Stream Temperature Regimes. *River Research and Applications*
708 32:896–906.

709 Mantua, N., I. Tohver, and A. Hamlet. 2010. Climate change impacts on streamflow extremes and summertime stream
710 temperature and their possible consequences for freshwater salmon habitat in Washington State. *Climatic*
711 *Change* 102:187–223.

712 Mauger, S., R. Shaftel, J. C. Leppi, and D. J. Rinella. 2017. Summer temperature regimes in southcentral Alaska
713 streams: watershed drivers of variation and potential implications for Pacific salmon. *Canadian Journal of*
714 *Fisheries and Aquatic Sciences* 74:702–715.

715 Mayer, T. D. 2012. Controls of summer stream temperature in the Pacific Northwest. *Journal of Hydrology* 475:323–
716 335.

717 McGill, L. M., J. R. Brooks, and E. A. Steel. 2021. Spatiotemporal dynamics of water sources in a mountain river
718 basin inferred through $\Delta^2\text{H}$ and $\Delta^{18}\text{O}$ of water. *Hydrological Processes* 35.

719 Meier, W., C. Bonjour, A. Wüest, and P. Reichert. 2003. Modeling the Effect of Water Diversion on the Temperature
720 of Mountain Streams. *Journal of Environmental Engineering* 129:755–764.

721 Menberg, K., P. Blum, B. L. Kurylyk, and P. Bayer. 2014. Observed groundwater temperature response to recent
722 climate change. *Hydrology and Earth System Sciences* 18:4453–4466.

723 Mohseni, O., T. R. Erickson, and H. G. Stefan. 1999. Sensitivity of stream temperatures in the United States to air
724 temperatures projected under a global warming scenario. *Water Resources Research* 35:3723–3733.

725 Mohseni, O., and H. G. Stefan. 1999. Stream temperature/air temperature relationship: a physical interpretation.
726 *Journal of Hydrology* 218:128–141.

727 Mohseni, O., H. G. Stefan, and J. G. Eaton. 2003. Global Warming and Potential Changes in Fish Habitat in U.S.
728 Streams. *Climatic Change* 59:389–409.

729 Mohseni, O., H. G. Stefan, and T. R. Erickson. 1998. A nonlinear regression model for weekly stream temperatures.
730 *Water Resources Research* 34:2685–2692.

731 Montgomery Water Group. 2003. Wenatchee River Basin Watershed Assessment.

732 Musselman, K. N., N. Addor, J. A. Vano, and N. P. Molotch. 2021. Winter melt trends portend widespread declines
733 in snow water resources. *Nature Climate Change* 11:418–424.

734 Neff, B. P., D. O. Rosenberry, S. G. Leibowitz, D. M. Mushet, H. E. Golden, M. C. Rains, J. R. Brooks, and C. R.
735 Lane. 2019. A Hydrologic Landscapes Perspective on Groundwater Connectivity of Depressional Wetlands.
736 *Water* 12:50.

737 Nelson, L. M. 1971. Sediment transport by streams in the Snohomish River basin, Washington: October 1967-
738 June 1969.

739 O’Driscoll, M. A., and D. R. DeWalle. 2006. Stream–air temperature relations to classify stream–ground water
740 interactions in a karst setting, central Pennsylvania, USA. *Journal of Hydrology* 329:140–153.

741 Olden, J. D., M. J. Kennard, and B. J. Pusey. 2012. A framework for hydrologic classification with a review of
742 methodologies and applications in ecohydrology: A FRAMEWORK FOR HYDROLOGIC
743 CLASSIFICATION. *Ecohydrology* 5:503–518.

744 Olden, J. D., J. J. Lawler, and N. L. Poff. 2008. Machine Learning Methods Without Tears: A Primer for Ecologists.
745 *The Quarterly Review of Biology* 83:171–193.

746 Ouellet, V., A. St-Hilaire, S. J. Dugdale, D. M. Hannah, S. Krause, and S. Proulx-Ouellet. 2020. River temperature
747 research and practice: Recent challenges and emerging opportunities for managing thermal habitat conditions
748 in stream ecosystems. *Science of The Total Environment* 736:139679.

749 Parkinson, E. A., E. V. Lea, M. A. Nelitz, J. M. Knudson, and R. D. Moore. 2016. Identifying Temperature Thresholds
750 Associated with Fish Community Changes in British Columbia, Canada, to Support Identification of
751 Temperature Sensitive Streams: STREAM TEMPERATURE AND FISH COMMUNITIES. *River Research
752 and Applications* 32:330–347.

753 Patton, N. R., K. A. Lohse, S. E. Godsey, B. T. Crosby, and M. S. Seyfried. 2018. Predicting soil thickness on soil
754 mantled hillslopes. *Nature Communications* 9:3329.

755 Pollock, M. M., T. J. Beechie, J. M. Wheaton, C. E. Jordan, N. Bouwes, N. Weber, and C. Volk. 2014. Using Beaver
756 Dams to Restore Incised Stream Ecosystems. *BioScience* 64:279–290.

757 Pyne, M. I., and N. L. Poff. 2017. Vulnerability of stream community composition and function to projected thermal
758 warming and hydrologic change across ecoregions in the western United States. *Global Change Biology*
759 23:77–93.

760 R Core Team. 2020. R: A Language and Environment for Statistical Computing. R Foundation for Statistical
761 Computing, Vienna, Austria.

762 Safeeq, M., G. S. Mauger, G. E. Grant, I. Arismendi, A. F. Hamlet, and S.-Y. Lee. 2014. Comparing Large-Scale
763 Hydrological Model Predictions with Observed Streamflow in the Pacific Northwest: Effects of Climate and
764 Groundwater*. *Journal of Hydrometeorology* 15:2501–2521.

765 Savoy, P., A. P. Appling, J. B. Heffernan, E. G. Stets, J. S. Read, J. W. Harvey, and E. S. Bernhardt. 2019. Metabolic
766 rhythms in flowing waters: An approach for classifying river productivity regimes. *Limnology and*
767 *Oceanography* 64:1835–1851.

768 Siegel, J. E., A. H. Fullerton, and C. E. Jordan. 2022. Accounting for snowpack and time-varying lags in statistical
769 models of stream temperature. *Journal of Hydrology X* 17:100136.

770 Snyder, C. D., N. P. Hitt, and J. A. Young. 2015. Accounting for groundwater in stream fish thermal habitat responses
771 to climate change. *Ecological Applications* 25:1397–1419.

772 Snyder, M. N., N. H. Schumaker, J. B. Dunham, M. L. Keefer, P. Leinenbach, A. Brookes, J. Palmer, J. Wu, D.
773 Keenan, and J. L. Ebersole. 2020. Assessing contributions of cold-water refuges to reproductive migration
774 corridor conditions for adult salmon and steelhead trout in the Columbia River, USA. *Journal of*
775 *Ecohydraulics*:1–13.

776 Soulsby, C., P. J. Rodgers, J. Petry, D. M. Hannah, I. A. Malcolm, and S. M. Dunn. 2004. Using tracers to upscale
777 flow path understanding in mesoscale mountainous catchments: two examples from Scotland. *Journal of*
778 *Hydrology* 291:174–196.

779 Steel, E. A., T. J. Beechie, C. E. Torgersen, and A. H. Fullerton. 2017. Envisioning, Quantifying, and Managing
780 Thermal Regimes on River Networks. *BioScience* 67:506–522.

781 Steel, E. A., A. Marsha, A. H. Fullerton, J. D. Olden, N. K. Larkin, S.-Y. Lee, and A. Ferguson. 2019. Thermal
782 landscapes in a changing climate: biological implications of water temperature patterns in an extreme year.
783 *Canadian Journal of Fisheries and Aquatic Sciences* 76:1740–1756.

784 Stefan, H. G., and B. A. Sinokrot. 1993. Projected global climate change impact on water temperatures in five north
785 central U.S. streams. *Climatic Change* 24:353–381.

786 Tague, C., M. Farrell, G. Grant, S. Lewis, and S. Rey. 2007. Hydrogeologic controls on summer stream temperatures
787 in the McKenzie River basin, Oregon. *Hydrological Processes* 21:3288–3300.

788 Therneau, T., and B. Atkinson. 2019. rpart: Recursive Partitioning and Regression Trees.

789 Thornton, M.M., Shrestha, R., Wei, Y., Thornton, P.E., Kao, S., and Wilson, B.E. 2020. DaymetDaymet: Daily
790 Surface Weather Data on a 1-km Grid for North America, Version 4:0 MB.

791 Turney, G. L., S. C. Kahle, and N. P. Dion. 1995. Geohydrology and ground-water quality of east King County,
792 Washington. Water Resources Investigations Report, Prepared in cooperation with Seattle-King County
793 Department of Health Tacoma, Washington, Washington, D. C.

794 Ver Hoef, J. M., and E. E. Peterson. 2010. A Moving Average Approach for Spatial Statistical Models of Stream
795 Networks. *Journal of the American Statistical Association* 105:6–18.

796 van Vliet, M. T. H., W. H. P. Franssen, J. R. Yearsley, F. Ludwig, I. Haddeland, D. P. Lettenmaier, and P. Kabat.
797 2013. Global river discharge and water temperature under climate change. *Global Environmental Change*
798 23:450–464.

799 van Vliet, M. T. H., F. Ludwig, J. J. G. Zwolsman, G. P. Weedon, and P. Kabat. 2011. Global river temperatures and
800 sensitivity to atmospheric warming and changes in river flow: SENSITIVITY OF GLOBAL RIVER
801 TEMPERATURES. *Water Resources Research* 47.

802 Webb, B. W., D. M. Hannah, R. D. Moore, L. E. Brown, and F. Nobilis. 2008. Recent advances in stream and river
803 temperature research. *Hydrological Processes* 22:902–918.

804 Webb, B. W., and F. Nobilis. 2007. Long-term changes in river temperature and the influence of climatic and
805 hydrological factors. *Hydrological Sciences Journal* 52:74–85.

806 Webb, B. W., and Y. Zhang. 1997. SPATIAL AND SEASONAL VARIABILITY IN THE COMPONENTS OF THE
807 RIVER HEAT BUDGET. *Hydrological Processes* 11:79–101.

808 Wildrick, L. 1979. Ground Water Flow System of the Chumstick Drainage Basin. Page 5. Washington State
809 Department of Ecology, Olympia, WA.

810 Winfree, M. M., E. Hood, S. L. Stuefer, D. E. Schindler, T. J. Cline, C. D. Arp, and S. Pyare. 2018. Landcover and
811 geomorphology influence streamwater temperature sensitivity in salmon bearing watersheds in Southeast
812 Alaska. *Environmental Research Letters* 13:064034.

813 Wolock, D. M., T. C. Winter, and G. McMahon. 2004. Delineation and Evaluation of Hydrologic-Landscape Regions
814 in the United States Using Geographic Information System Tools and Multivariate Statistical Analyses.
815 *Environmental Management* 34:S71–S88.

816 Wondzell, S. M., M. Diabat, and R. Haggerty. 2019. What Matters Most: Are Future Stream Temperatures More
817 Sensitive to Changing Air Temperatures, Discharge, or Riparian Vegetation? JAWRA Journal of the
818 American Water Resources Association 55:116–132.

819 Wu, H., J. S. Kimball, M. M. Elsner, N. Mantua, R. F. Adler, and J. Stanford. 2012. Projected climate change impacts
820 on the hydrology and temperature of Pacific Northwest rivers: CLIMATE CHANGE IMPACTS ON
821 STREAMFLOW AND TEMPERATURE. Water Resources Research 48.

822 Yan, H., N. Sun, A. Fullerton, and M. Baerwalde. 2021. Greater vulnerability of snowmelt-fed river thermal regimes
823 to a warming climate. Environmental Research Letters 16:054006.

824

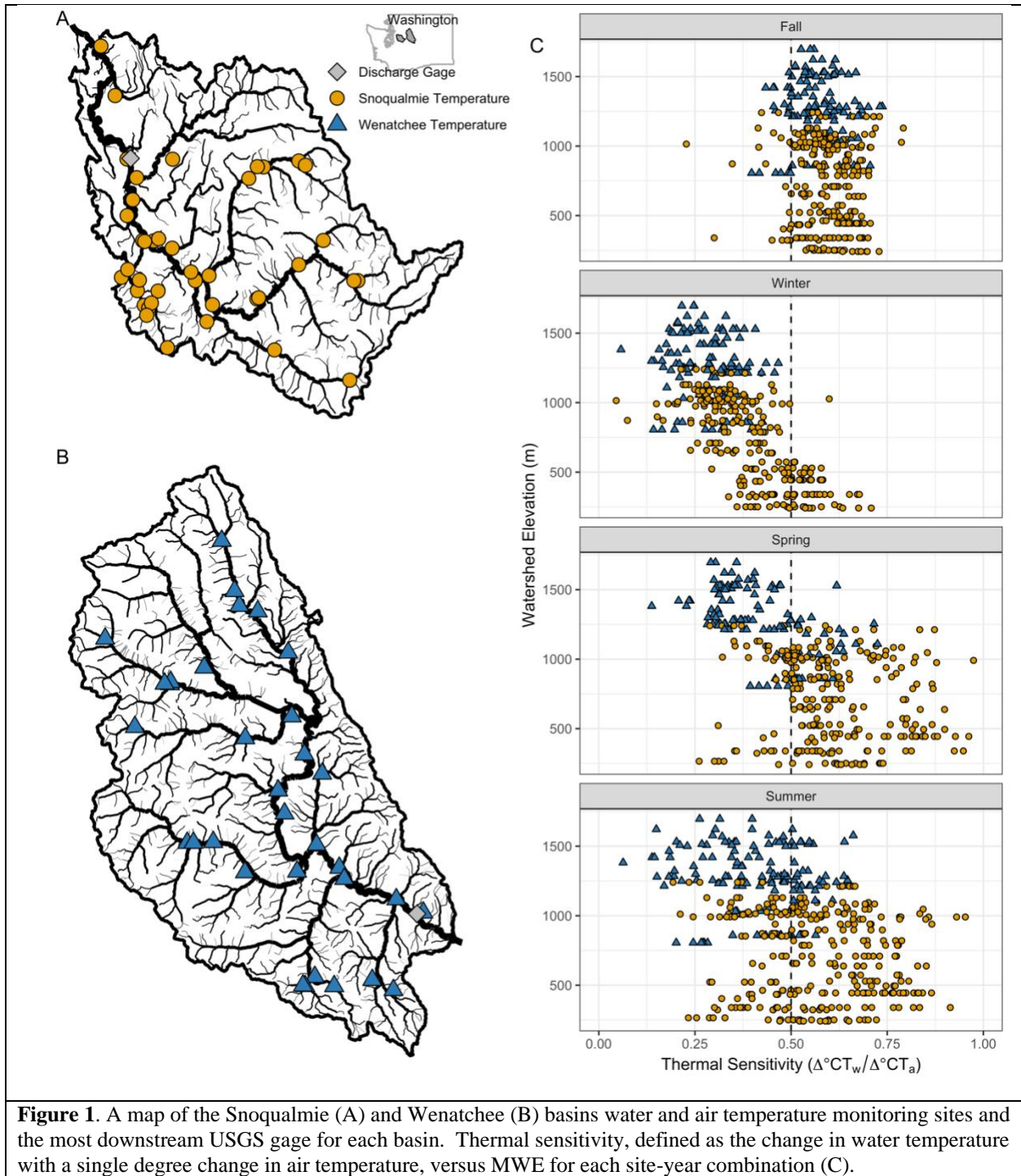


Figure 1. A map of the Snoqualmie (A) and Wenatchee (B) basins water and air temperature monitoring sites and the most downstream USGS gage for each basin. Thermal sensitivity, defined as the change in water temperature with a single degree change in air temperature, versus MWE for each site-year combination (C).

825

826

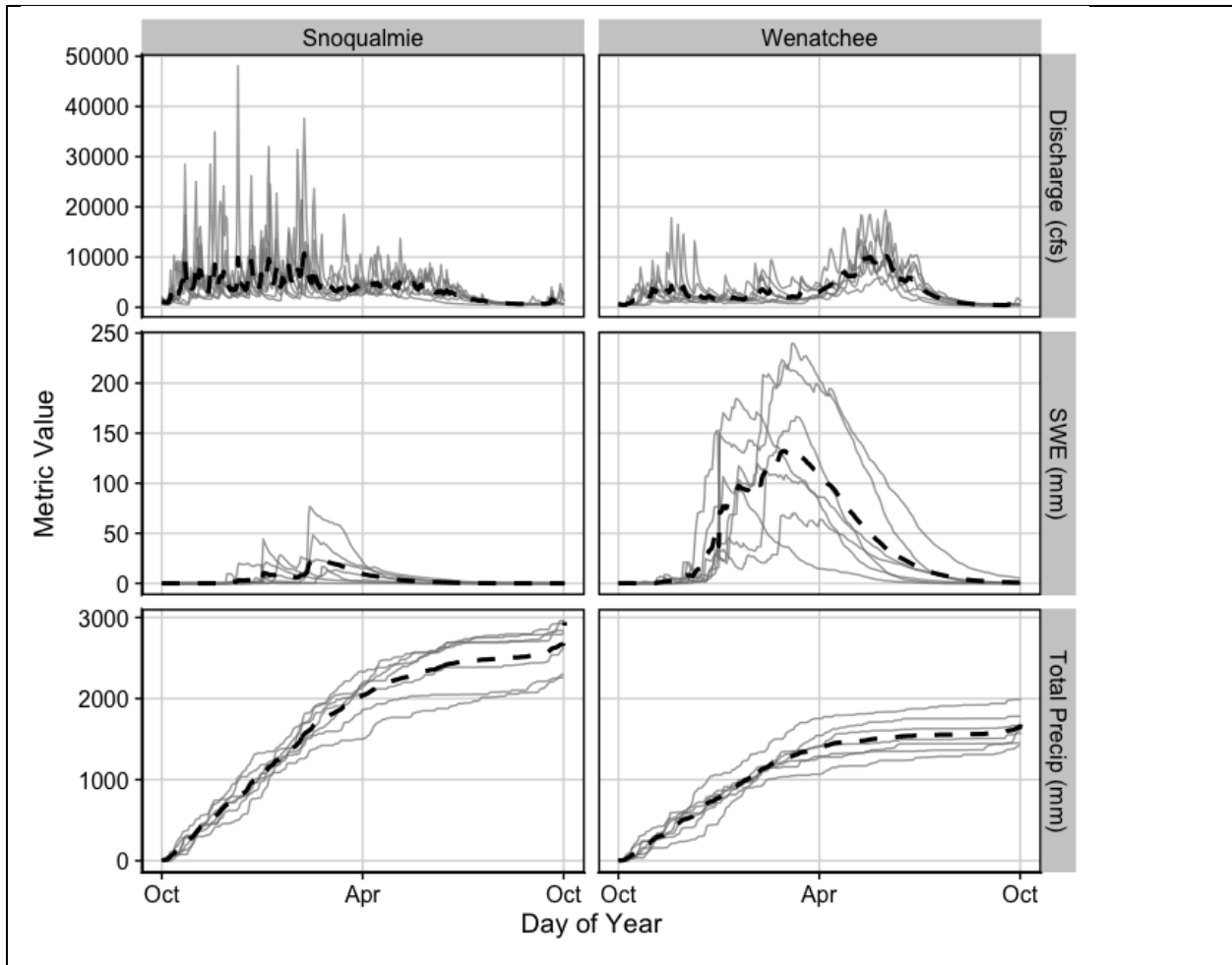


Figure 2. Average annual discharge, SWE, and total precipitation for the Snoqualmie and Wenatchee basins across the sampling timeframe (black dashed lines) and interannual variability across the seven water years included in this analysis (gray lines).

828

829

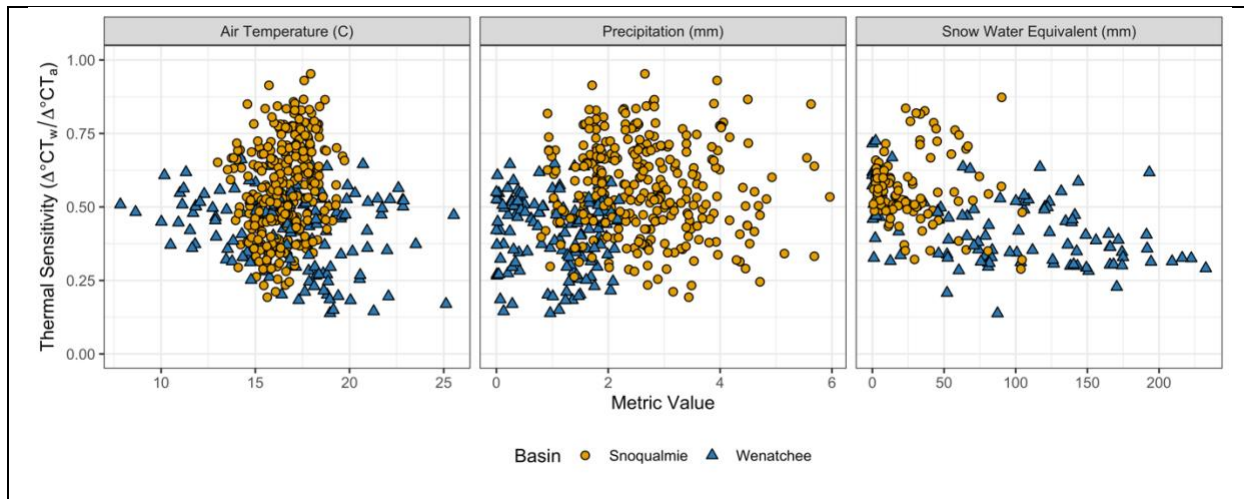


Figure 3. Summer thermal sensitivity values for all site-year combinations in the Snoqualmie and Wenatchee basins versus air temperature (A), and precipitation (B). Spring thermal sensitivity values for all site-year combinations versus total SWE (C) from gridded DAYMET data for each sampling point. Points are colored by basin. Basins that have no snowmelt in a given year are not shown on graph (C).

830

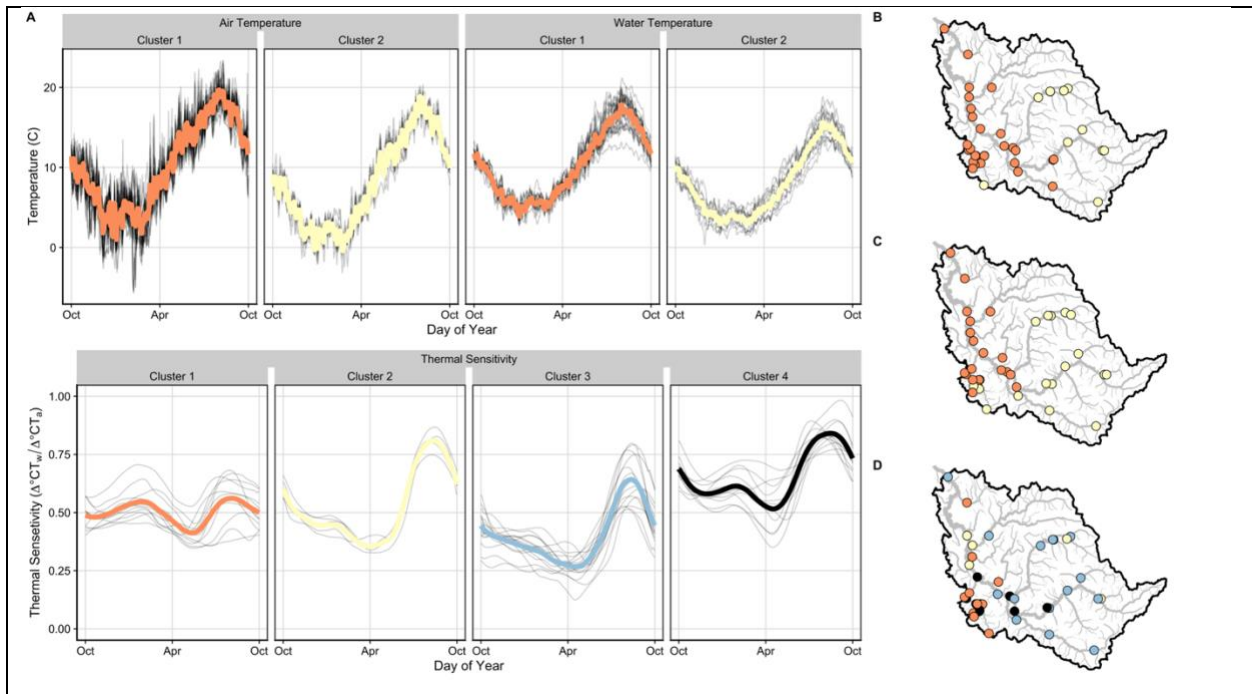


Figure 4. Average time series (A) and spatial clustering results (columns/colors indicate unique clusters) for average annual air temperature (B), water temperature (C), and thermal sensitivity (D) in the Snoqualmie basin. The spatial distribution for colored lines indicates mean average annual values for each cluster, and gray lines denote average annual values for each site within a given cluster.

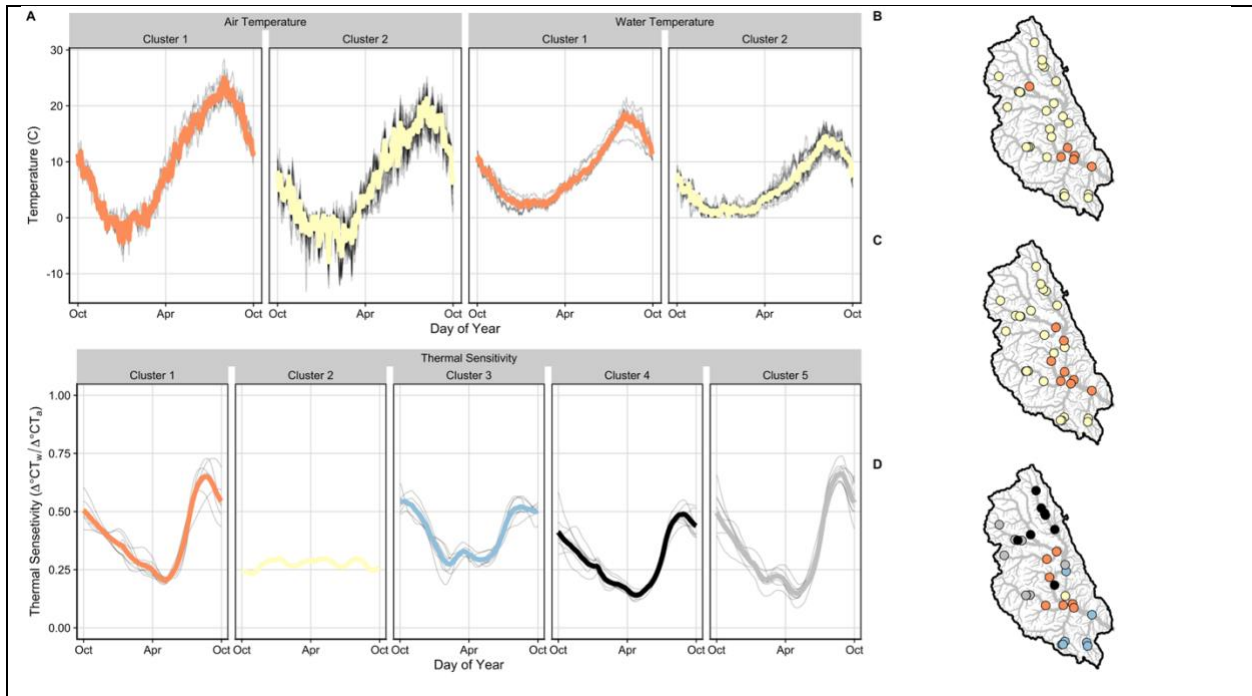


Figure 5. Average time series (A) and spatial clustering results (columns/colors indicate unique clusters) for average annual air temperature (B), water temperature (C), and thermal sensitivity (D) in the Wenatchee basin. The spatial distribution for colored lines indicates mean average annual values for each cluster, and gray lines denote average annual values for each site within a given cluster.

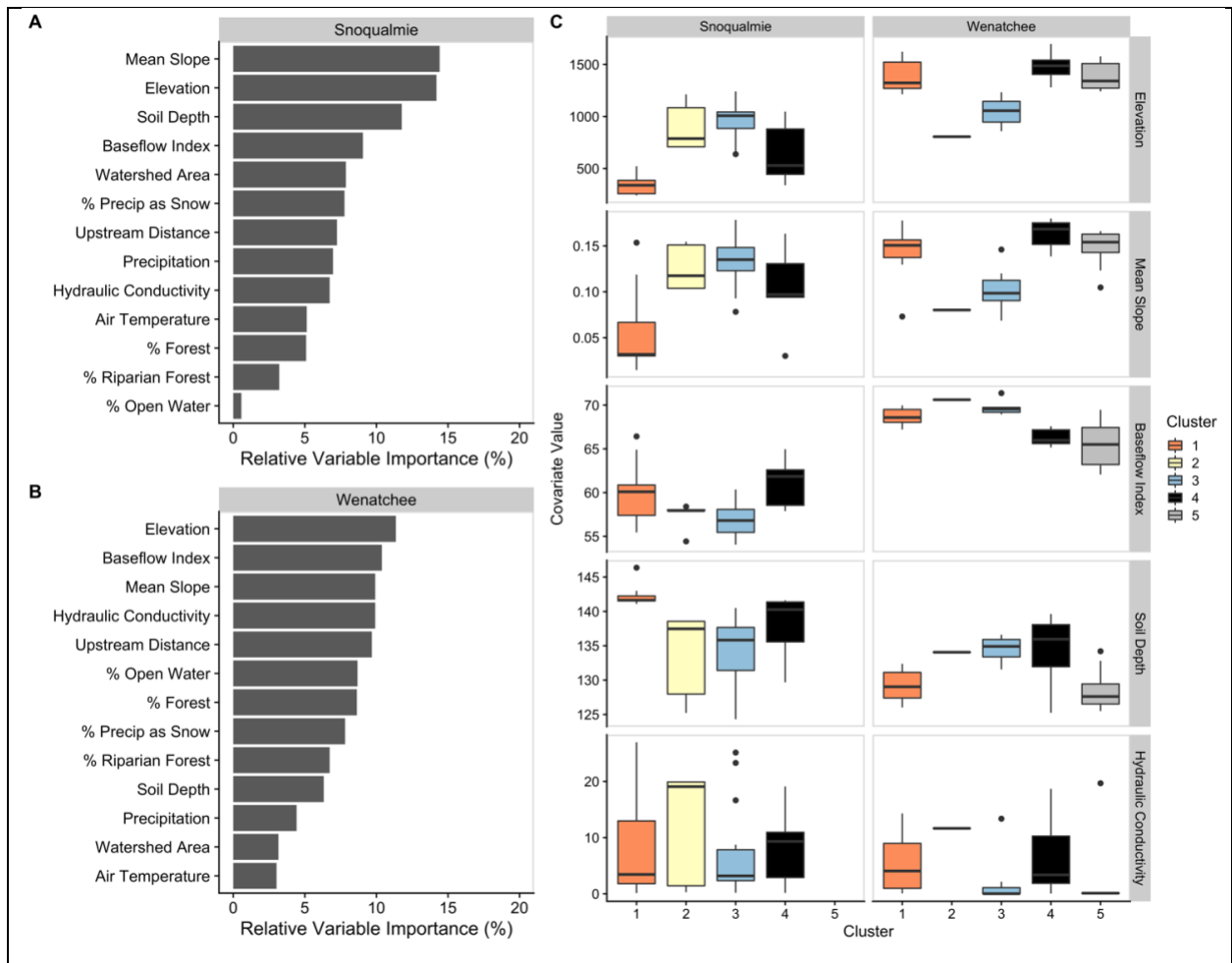


Figure 6. Relative variable importance for all covariates in the Snoqualmie (A) Wenatchee (B) basins, and the distributions of variables for the four most important variables (C) in the Snoqualmie basin (Mean Slope, Elevation, Soil Depth, and Baseflow Index) and in the Wenatchee basin (Elevation, Baseflow Index, Mean Slope, and Hydraulic Conductivity). Boxes are grouped and colored by cluster membership. See Figure S7 for plots of the remaining relative variable importances.

Table 1. Physical environmental data and basin characteristics used to predict air-water clusters.

Variable	Category	Units	Data Source
Watershed area	Basin Topography	km ²	Hill et al. 2016
Mean watershed elevation	Basin Topography	m	Hill et al. 2016
Avg. stream slope	Basin Topography	mm ⁻¹	Hill et al. 2016
Distance upstream	Basin Topography	km	Hill et al. 2016
% Watershed forest	Land Use	%	Hill et al. 2016; Dewitz et al. 2019
% Riparian forest	Land Use	%	Hill et al. 2016; Dewitz et al. 2019
% Lake area	Land Use	%	Hill et al. 2016; Dewitz et al. 2019
Avg. Temperature	Climate	C	Hart and Bell 2015
Avg. Precipitation	Climate	mm	Hart and Bell 2015
Avg. % precip as snow	Climate	%	Hart and Bell 2015
Baseflow index	Hydrogeologic	%	Hill et al. 2016; Wolock 2003
Hydraulic conductivity	Hydrogeologic	%	Hill et al. 2016; Olson and Hawkins 2014
Soil depth to bedrock	Hydrogeologic	cm	Hill et al. 2016; Carlisle et al. 2009

5

Table 2. Air water correlation summary metrics by basin and season.

		Thermal Sensitivity			R ²		
		Min	Mean	Max	Min	Mean	Max
Snoqualmie	Fall	0.22	0.59	0.79	0.58	0.92	0.99
	Winter	0.05	0.40	0.71	0.20	0.86	0.96
	Spring	0.26	0.60	0.97	0.67	0.89	0.98
	Summer	0.19	0.56	0.95	0.41	0.85	0.97
Wenatchee	Fall	0.40	0.57	0.74	0.74	0.94	0.98
	Winter	0.05	0.28	0.47	0.44	0.84	0.95
	Spring	0.14	0.42	0.72	0.59	0.88	0.98
	Summer	0.06	0.41	0.66	0.08	0.77	0.96

10 **Table 3.** Hypothesized relationships between landscape covariates and thermal sensitivity based on previous literature (A) and the observed relationship between landscape variables and thermal sensitivities within our study basins in summer (B). Loess curves are shown to aid in visualization and correlation coefficients quantify the strength of the linear relationship. See Figure S6 for a detailed description of how river attributes covary with one another.

15

A. Hypothesized Drivers			B. Observed Relationship
Stream or watershed attribute (covarying variables)	Theoretical relationship with thermal sensitivity	Explanation	Observed Relationship in Summer
Mean watershed slope +elevation +dist upstream – soil depth	Negative	<ul style="list-style-type: none"> Increased snowmelt and cooling due to faster velocity water movement and shorter water residence time (Winfree et al. 2018). Topographic shading associated with steep watersheds suppresses stream temperature by reducing exposure to solar radiation (Webb and Zhang 1997). 	
Mean watershed elevation +slope +dist upstream +% lake area – soil depth	Negative	<ul style="list-style-type: none"> Higher elevations have higher snowmelt accumulation and greater proportion of snowmelt in spring. The impact of elevation on spring and early summer stream temperature is diminished in years with low winter snow accumulation. 	
Distance upstream – watershed size +slope +elevation	Negative	<ul style="list-style-type: none"> Duration of surface water's exposure to solar radiation and atmospheric energy flux is higher in low gradient watersheds with slower streamflow velocities (Poole and Berman 2001). 	
Percent riparian forest cover +% forest cover – watershed size	Negative	<ul style="list-style-type: none"> Riparian vegetation provides shading to streams, reducing exposure to solar radiation (Webb and Zhang 1997), particularly during summer base flows. Forest canopy can influence snow accumulation within a watershed and snowmelt contribution to streams. Low density forests accumulate more snow relative to 	

		<p>high density forests (Varhola et al 2010).</p> <ul style="list-style-type: none"> • Conversion of forested land area can accelerate runoff and reduce infiltration, warming surface flows before they reach stream channels (Naiman et al. 2005; Nelson and Palmer 2007). 	
<p>Hydraulic Conductivity +baseflow index</p>	<p>Positive</p>	<ul style="list-style-type: none"> • Hydraulic conductivity refers to the ability of a geologic material to transmit water. • Relatively high hydraulic conductivity material would be represented by something like unconsolidated alluvial sands and gravels. • High hydraulic conductivity is typically associated with areas of greater groundwater activity and lower, more stable thermal sensitivity values. 	

Table 4. Averaged metrics for all sites within each cluster determined with the spatially weighted agglomerative hierarchical clustering. For timing metrics, days are reported as hydrologic day, where a value of 1 indicates October 1st and a value of 365 indicates September 30th.

Metric	Basin	Cluster	# Sites	Mean	Minimum (timing)	Maximum (timing)	Cluster Stability
Thermal Sensitivity	Snoqualmie	1	11	0.50	0.41 (224)	0.56 (308)	0.68
		2	5	0.52	0.36 (181)	0.81 (315)	0.88
		3	15	0.40	0.27 (201)	0.64 (316)	0.67
		4	11	0.65	0.52 (199)	0.84 (316)	0.55
	Wenatchee	1	7	0.39	0.20 (216)	0.65 (324)	0.79
		2	1	0.27	0.23 (28)	0.30 (101)	0.62
		3	7	0.40	0.27 (131)	0.54 (11)	0.94
		4	8	0.29	0.14 (207)	0.48 (331)	0.86
		5	8	0.35	0.15 (214)	0.66 (330)	0.69
	Air	Snoqualmie	1	31	10.2	1.01 (94)	19.7 (305)
2			11	8.02	-0.42 (145)	18.9 (304)	0.73
Wenatchee		1	6	9.68	-4.52 (95)	25.0 (304)	0.95
		2	25	6.48	-7.88 (107)	21.3 (310)	0.85
Water	Snoqualmie	1	25	10.1	3.91 (94)	17.8 (304)	0.65
		2	17	7.99	2.94 (94)	15.6 (304)	0.89
	Wenatchee	1	8	8.39	1.95 (108)	18.5 (310)	0.73
		2	23	5.74	0.37 (107)	14.5 (310)	0.86